The Mu2e Experiment
Search for Charged Lepton Flavour Violation

Fermilab 2024 Summer Students School
(The Italian Summer Student Program)

Namitha Chithirasreemadam
namithac@pi.infn.it

Dipartimento di Fisica 'Enrico Fermi'
Università di Pisa,
INFN, Pisa

24 July 2024

H2020 MSCA ITN
G.A. 858199

Charged Lepton Flavour Violation (CLFV)

Charged Lepton Flavour Violation (CLFV)

- Flavour is not conserved in:
  -> quarks
  -> neutrinos
  -> charged leptons?

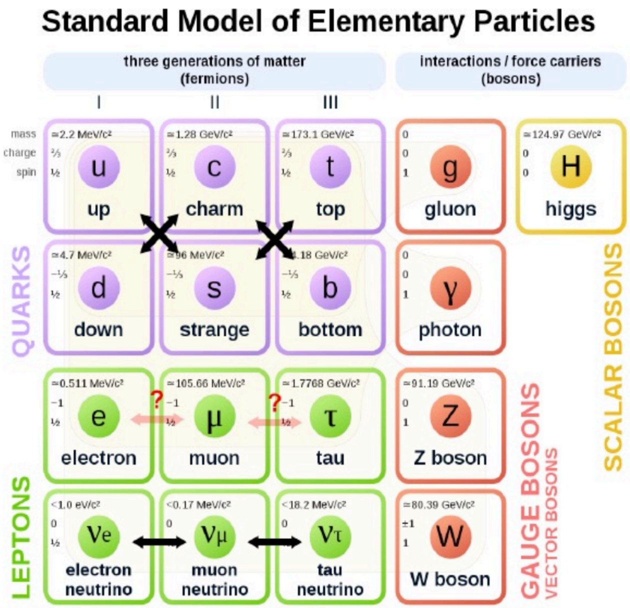

Charged Lepton Flavour Violation (CLFV)

- Flavour is not conserved in:
  -> quarks
  -> neutrinos
  -> charged leptons?

- CLFV can occur through neutrino oscillation, mediated by W bosons.

$$B(\mu \rightarrow e\gamma) = \frac{3\alpha}{32\pi}(\frac{1}{4})sin^2 2\theta_{13} sin^2\theta_{23} | \frac{\Delta m^2_{13}}{M^2_W} |^2$$

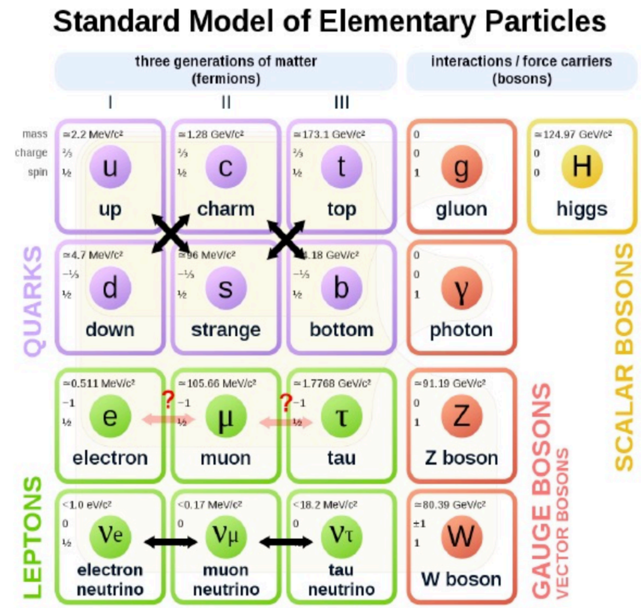

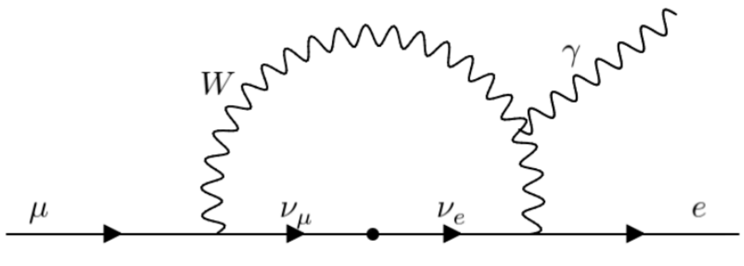

Charged Lepton Flavour Violation (CLFV)

- Flavour is not conserved in:
  -> quarks
  -> neutrinos
  -> charged leptons?

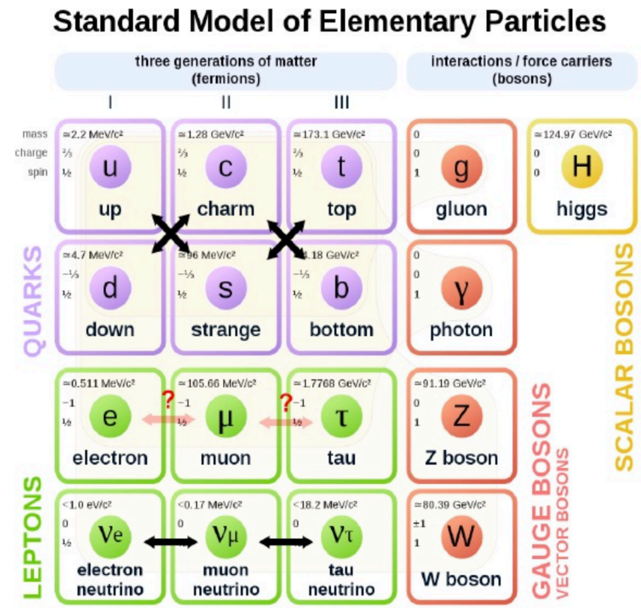

- CLFV can occur through neutrino oscillation, mediated by W bosons.

$$B(\mu \to e\gamma) = \frac{3\alpha}{32\pi}\left(\frac{1}{4}\right)sin^2 2\theta_{13} sin^2\theta_{23} \left|\frac{\Delta m^2_{13}}{M^2_W}\right|^2$$

- Branching fractions of CLFV processes through neutrino oscillations are suppressed by factors proportional to $(\Delta m^2_\nu)^2/M^4_W$ to **undetectably tiny** levels, $< 10^{-50}$.

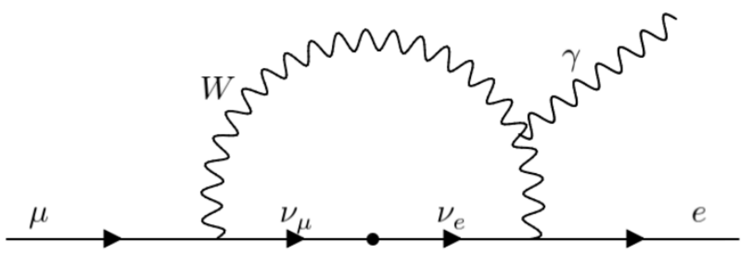

Charged Lepton Flavour Violation (CLFV)

Charged Lepton Flavour Violation (CLFV)

- Many New Physics models (SO(10) SUSY, scalar leptoquarks, seesaw model) predict much enhanced rates of CLFV O(10^{-13}).

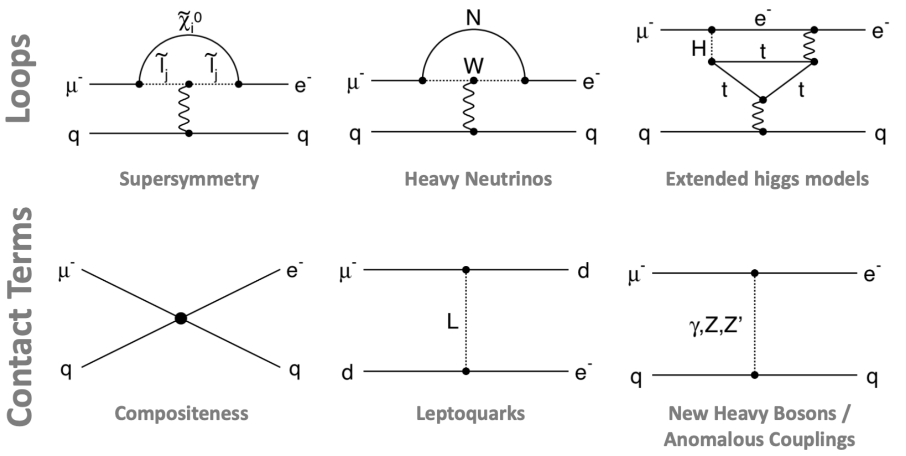

Charged Lepton Flavour Violation (CLFV)

- Many New Physics models (SO(10) SUSY, scalar leptoquarks, seesaw model) predict much enhanced rates of CLFV O(10^{-13}).

- In the EFT Lagrangian parameterisation, Λ is the effective mass scale and κ controls the relative contribution of the dipole moment term and the four fermion term.

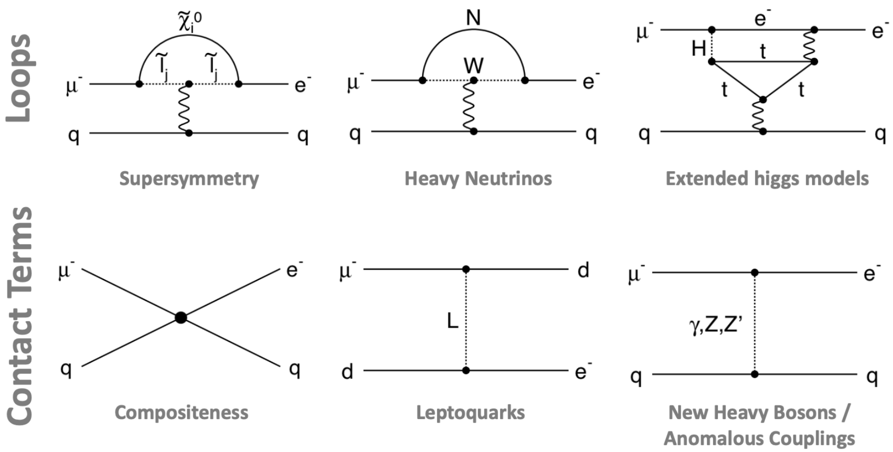

$$\mathscr{L}_{CLFV} = \frac{m_\mu}{(1+\kappa)\Lambda^2}\bar{\mu}_R\sigma_{\mu\nu}e_L F^{\mu\nu} + \frac{\kappa}{1+\kappa}\bar{\mu}_L\gamma_\mu e_L \sum_{q=u,d}\overline{q_L}\gamma^\mu q_L$$

Charged Lepton Flavour Violation (CLFV)

- Many New Physics models (SO(10) SUSY, scalar leptoquarks, seesaw model) predict much enhanced rates of CLFV O(10^{-13}).

- In the EFT Lagrangian parameterisation, Λ is the effective mass scale and κ controls the relative contribution of the dipole moment term and the four fermion term.

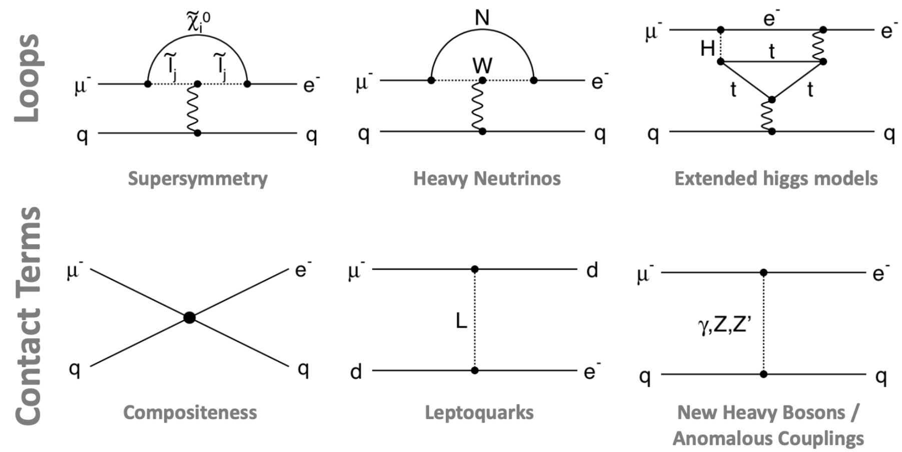

$$\mathscr{L}_{CLFV} = \frac{m_\mu}{(1+\kappa)\Lambda^2}\bar{\mu}_R\sigma_{\mu\nu}e_L F^{\mu\nu} + \frac{\kappa}{1+\kappa}\bar{\mu}_L\gamma_\mu e_L \sum_{q=u,d}\overline{q_L}\gamma^\mu q_L$$

Dipole term:

$\mu^+ \to e^+\gamma, \mu^+ \to e^+e^+e^-$

$\mu^- N \to e^- N$ at loop level

Charged Lepton Flavour Violation (CLFV)

- Many New Physics models (SO(10) SUSY, scalar leptoquarks, seesaw model) predict much enhanced rates of CLFV O(10^{-13}).
- In the EFT Lagrangian parameterisation, Λ is the effective mass scale and κ controls the relative contribution of the dipole moment term and the four fermion term.

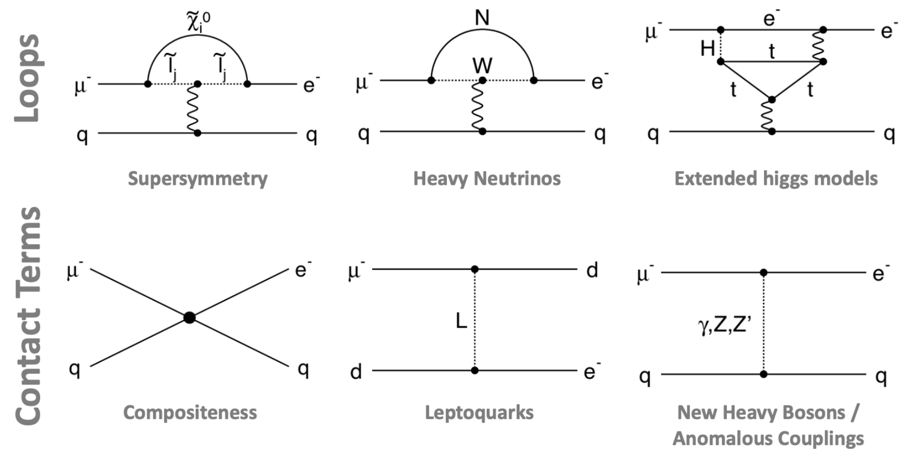

$$\mathscr{L}_{CLFV} = \frac{m_\mu}{(1+\kappa)\Lambda^2}\bar{\mu}_R\sigma_{\mu\nu}e_L F^{\mu\nu} + \frac{\kappa}{1+\kappa}\bar{\mu}_L\gamma_\mu e_L \sum_{q=u,d}\overline{q_L}\gamma^\mu q_L$$

Dipole term:
$\mu^+ \to e^+\gamma, \mu^+ \to e^+e^+e^-$
$\mu^- N \to e^- N$ at loop level

4 Fermion term:
$\mu^- N \to e^- N$ at leading order
Heavily suppressed in $\mu^+ \to e^+\gamma$

Charged Lepton Flavour Violation (CLFV)

- Many New Physics models (SO(10) SUSY, scalar leptoquarks, seesaw model) predict much enhanced rates of CLFV O(10^{-13}).

- In the EFT Lagrangian parameterisation, Λ is the effective mass scale and κ controls the relative contribution of the dipole moment term and the four fermion term.

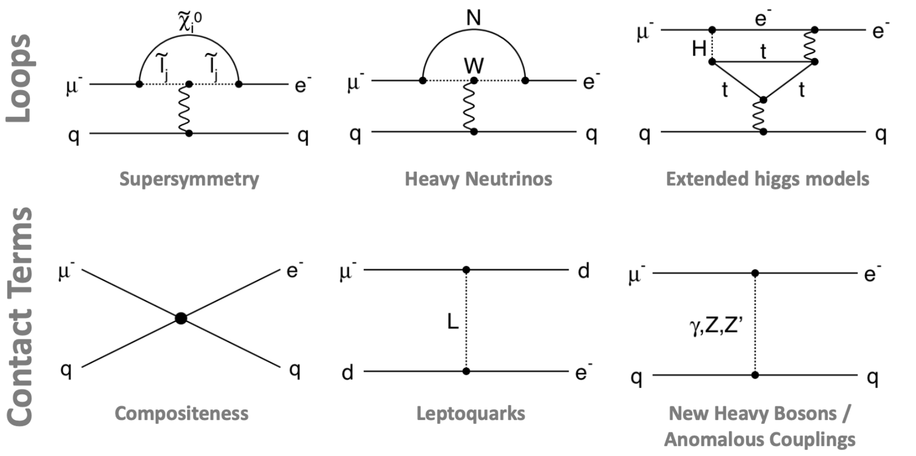

$$\mathscr{L}_{CLFV} = \frac{m_\mu}{(1+\kappa)\Lambda^2}\bar{\mu}_R \sigma_{\mu\nu} e_L F^{\mu\nu} + \frac{\kappa}{1+\kappa}\bar{\mu}_L \gamma_\mu e_L \sum_{q=u,d} \overline{q_L}\gamma^\mu q_L$$

Dipole term:
$\mu^+ \to e^+\gamma, \mu^+ \to e^+e^+e^-$
$\mu^- N \to e^- N$ at loop level

4 Fermion term:
$\mu^- N \to e^- N$ at leading order
Heavily suppressed in $\mu^+ \to e^+\gamma$

Observation of a CLFV process would be unambiguous evidence of New Physics

CLFV search through muons

CLFV search through muons

- Muons are powerful probe thanks to the availability of very intense beams and their relatively long lifetime.

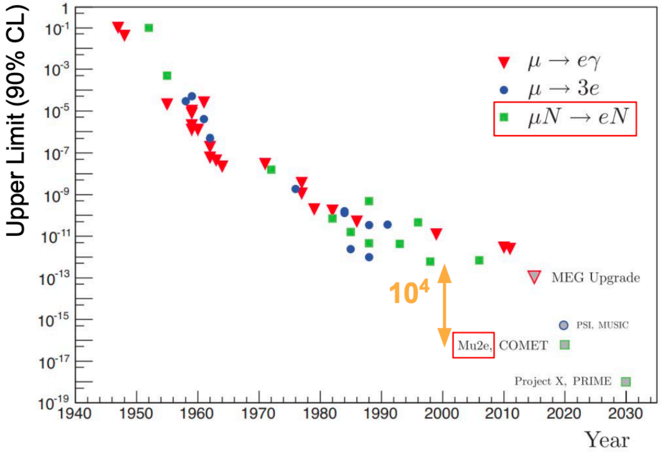

CLFV search through muons

- Muons are powerful probe thanks to the availability of very intense beams and their relatively long lifetime.

- The $\mu^- N \rightarrow e^- N$ conversion channel:
  -> No combinatorial background.
  -> Best sensitivity to CLFV in a large range of NP scenarios.
  -> Can give unique information regarding underlying NP operators.

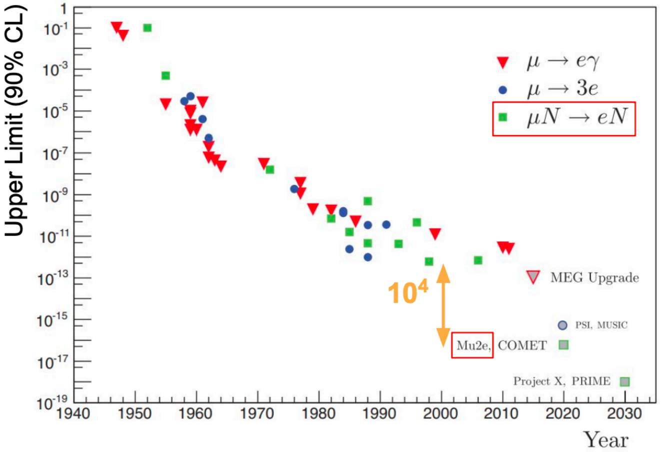

* Mu2e-II and AMF are proposed future experiments/facilities.

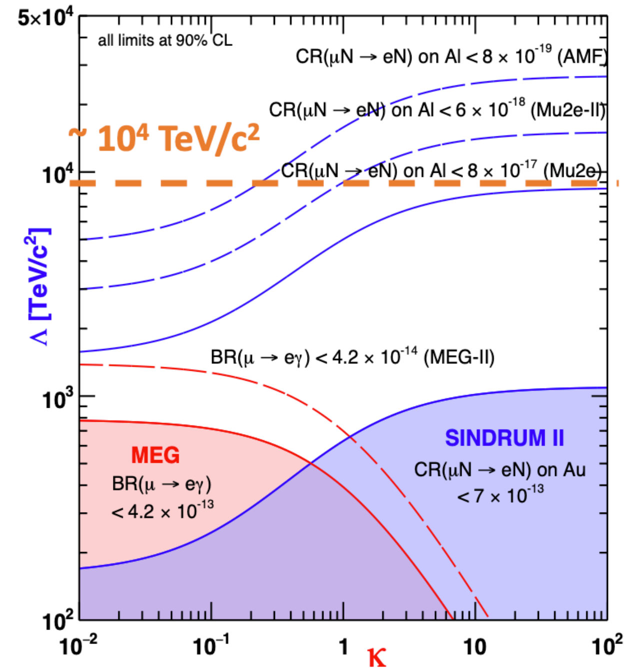

CLFV search through muons

- Muons are powerful probe thanks to the availability of very intense beams and their relatively long lifetime.

- The $\mu^- N \rightarrow e^- N$ conversion channel:
  -> No combinatorial background.
  -> Best sensitivity to CLFV in a large range of NP scenarios.
  -> Can give unique information regarding underlying NP operators.

- Current best limit on $\mu^- N \rightarrow e^- N$ set by SINDRUM II experiment: $R_{\mu e} < 7 \times 10^{-13}$ (90% C.L).

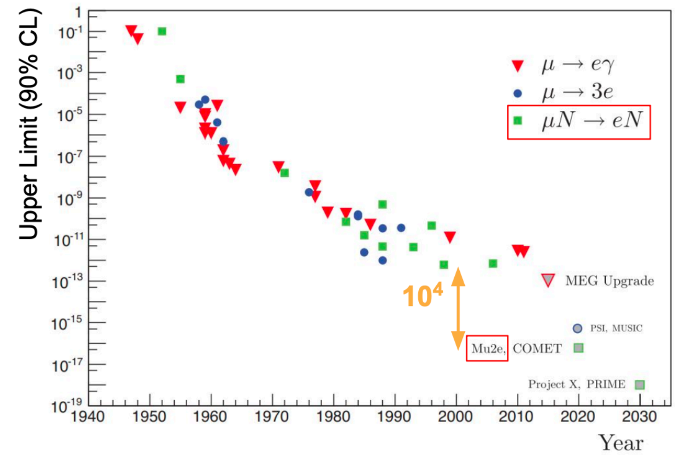

* Mu2e-II and AMF are proposed future experiments/facilities.

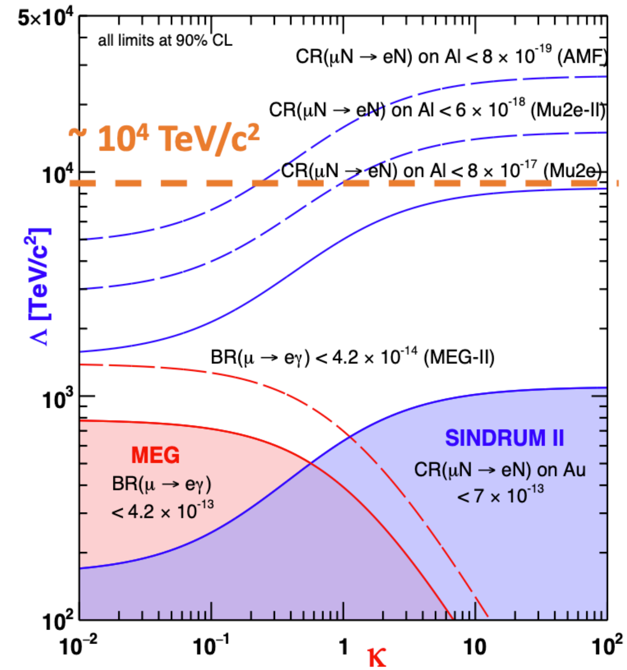

CLFV search through muons

- Muons are powerful probe thanks to the availability of very intense beams and their relatively long lifetime.
- The $\mu^- N \to e^- N$ conversion channel:
  -> No combinatorial background.
  -> Best sensitivity to CLFV in a large range of NP scenarios.
  -> Can give unique information regarding underlying NP operators.
- Current best limit on $\mu^- N \to e^- N$ set by SINDRUM II experiment: $R_{\mu e} < 7 \times 10^{-13}$ (90% C.L).
- Most stringent constraint on NP theories set by the MEG experiment
  BR($\mu^+ \to e^+ \gamma$) $< 4.2 \times 10^{-13}$ (90% C.L).

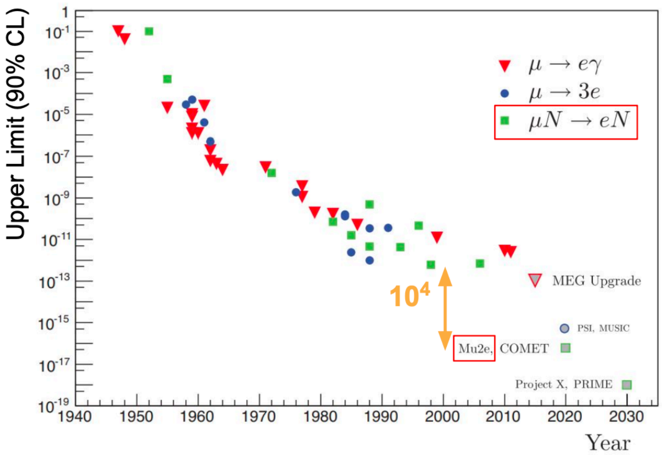

* Mu2e-II and AMF are proposed future experiments/facilities.

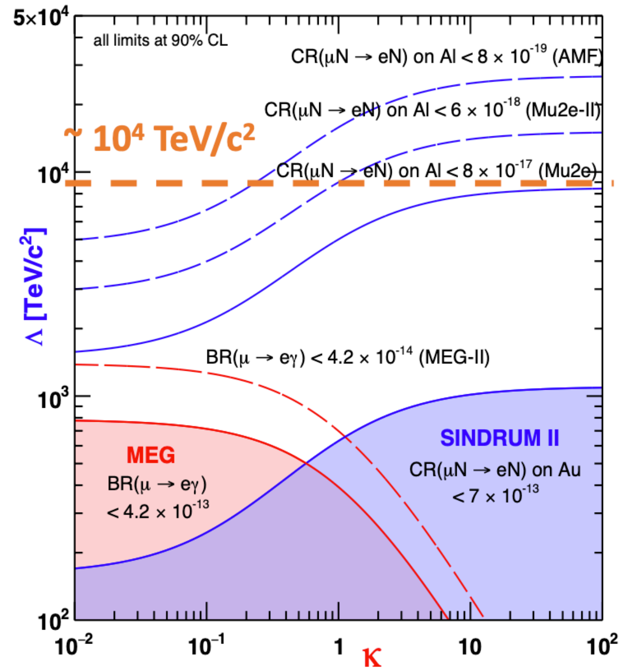

Mu2e: Muon-to-electron conversion

Mu2e: Muon-to-electron conversion

- Search for neutrinoless, coherent conversion $\mu^- N \rightarrow e^- N$ in the field of an Aluminum nucleus.

$$R_{\mu e} = \frac{\Gamma(\mu^- + N(Z,A) \rightarrow e^- + N(Z,A))}{\Gamma(\mu^- + N(Z,A) \rightarrow \nu_\mu + N(Z-1,A))}$$

Mu2e: Muon-to-electron conversion

- Search for neutrinoless, coherent conversion $\mu^- N \rightarrow e^- N$ in the field of an Aluminum nucleus.

- Low momentum muons are captured in the target atomic orbit and quickly (~fs) cascade to 1s state.

$$R_{\mu e} = \frac{\Gamma(\mu^- + N(Z,A) \rightarrow e^- + N(Z,A))}{\Gamma(\mu^- + N(Z,A) \rightarrow \nu_\mu + N(Z-1,A))}$$

Mu2e: Muon-to-electron conversion

- Search for neutrinoless, coherent conversion $\mu^- N \rightarrow e^- N$ in the field of an Aluminum nucleus.

- Low momentum muons are captured in the target atomic orbit and quickly (~fs) cascade to 1s state.

- In Aluminum,
  -> 39% Decay: $\mu N \rightarrow e + \bar{\nu}_e + \nu_\mu$ (Background)
  -> 61% Capture: $\mu N \rightarrow \nu_\mu N'$ (Normalisation)

$$R_{\mu e} = \frac{\Gamma(\mu^- + N(Z,A) \rightarrow e^- + N(Z,A))}{\Gamma(\mu^- + N(Z,A) \rightarrow \nu_\mu + N(Z-1,A))}$$

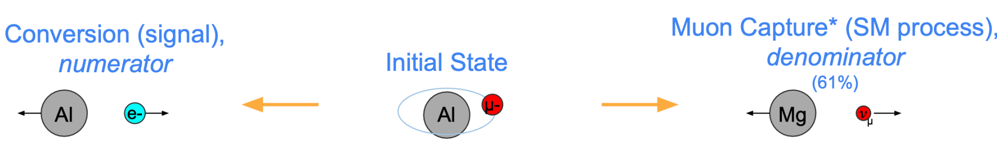

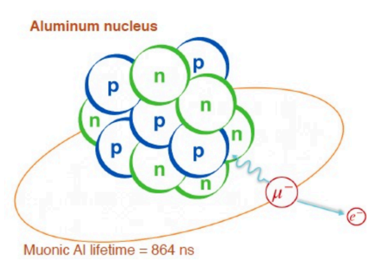

Mu2e: Muon-to-electron conversion

- Search for neutrinoless, coherent conversion $\mu^- N \rightarrow e^- N$ in the field of an Aluminum nucleus.

- Low momentum muons are captured in the target atomic orbit and quickly (~fs) cascade to 1s state.

- In Aluminum,
  -> 39% Decay: $\mu N \rightarrow e + \bar{\nu}_e + \nu_\mu$ (Background)
  -> 61% Capture: $\mu N \rightarrow \nu_\mu N'$ (Normalisation)

- Signal: Monochromatic conversion electron (CE) with energy

$$E_{CE} = m_\mu - E_{bind} - E_{recoil}$$

where m_μ is the muon mass, E_{bind} is the binding energy of the 1s state of the muonic atom, E_{recoil} is the recoil energy of the target nucleus.

$$R_{\mu e} = \frac{\Gamma(\mu^- + N(Z,A) \rightarrow e^- + N(Z,A))}{\Gamma(\mu^- + N(Z,A) \rightarrow \nu_\mu + N(Z-1,A))}$$

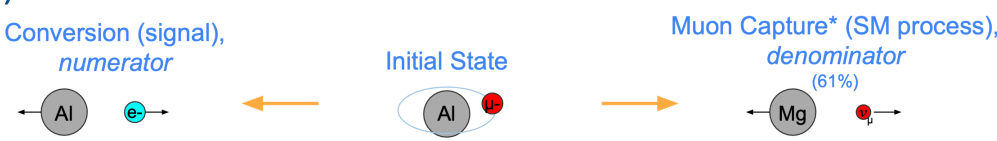

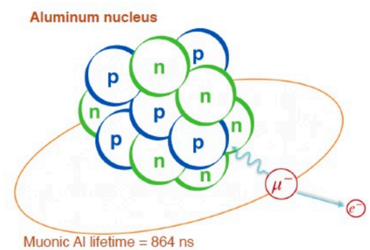

Mu2e: Muon-to-electron conversion

- Search for neutrinoless, coherent conversion $\mu^- N \rightarrow e^- N$ in the field of an Aluminum nucleus.

$$R_{\mu e} = \frac{\Gamma(\mu^- + N(Z,A) \rightarrow e^- + N(Z,A))}{\Gamma(\mu^- + N(Z,A) \rightarrow \nu_\mu + N(Z-1,A))}$$

- Low momentum muons are captured in the target atomic orbit and quickly (~fs) cascade to 1s state.

- In Aluminum,
  -> 39% Decay: $\mu N \rightarrow e + \bar{\nu}_e + \nu_\mu$ (Background)
  -> 61% Capture: $\mu N \rightarrow \nu_\mu N'$ (Normalisation)

- Signal: Monochromatic conversion electron (CE) with energy

$$E_{CE} = m_\mu - E_{bind} - E_{recoil}$$

where m_μ is the muon mass, E_{bind} is the binding energy of the 1s state of the muonic atom, E_{recoil} is the recoil energy of the target nucleus.

- For the Al target, $E_{CE} = 104.97$ MeV*.

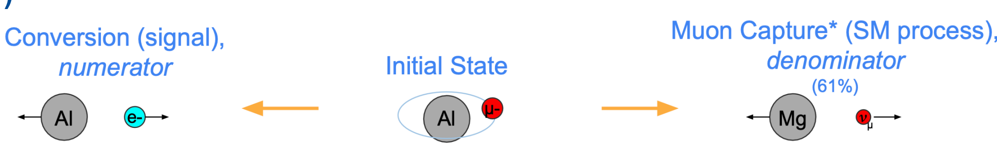

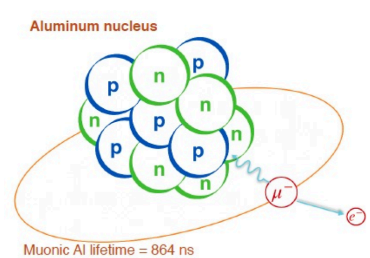

*https://link.aps.org/accepted/10.1103/PhysRevD.84.013006

Mu2e Experimental Setup

Mu2e Experimental Setup

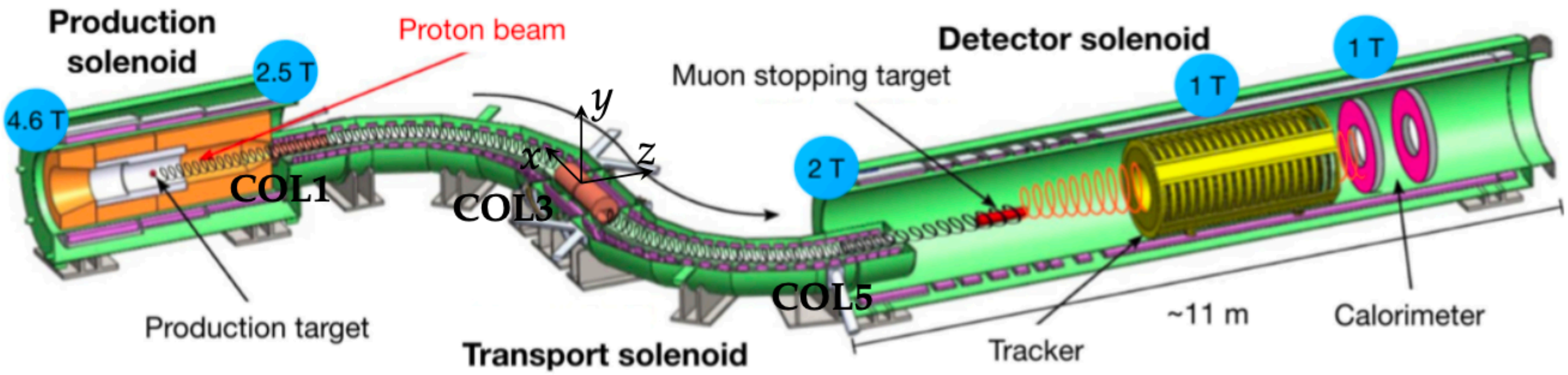

Mu2e Experimental Setup

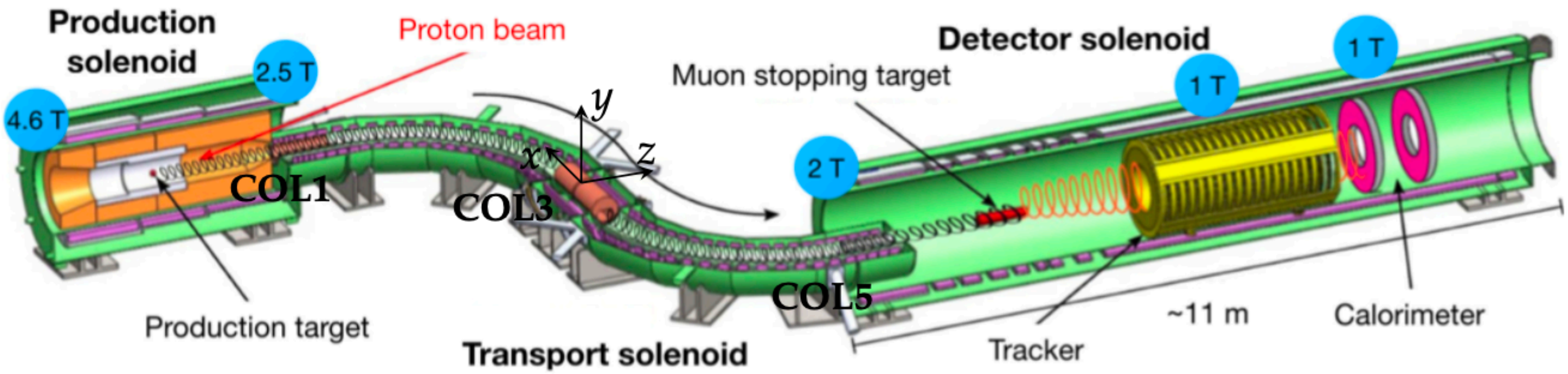

Production Solenoid

8 GeV pulsed proton beam interacts with the Tungsten target.

Mostly produces pions, decay into muons.

Mu2e Experimental Setup

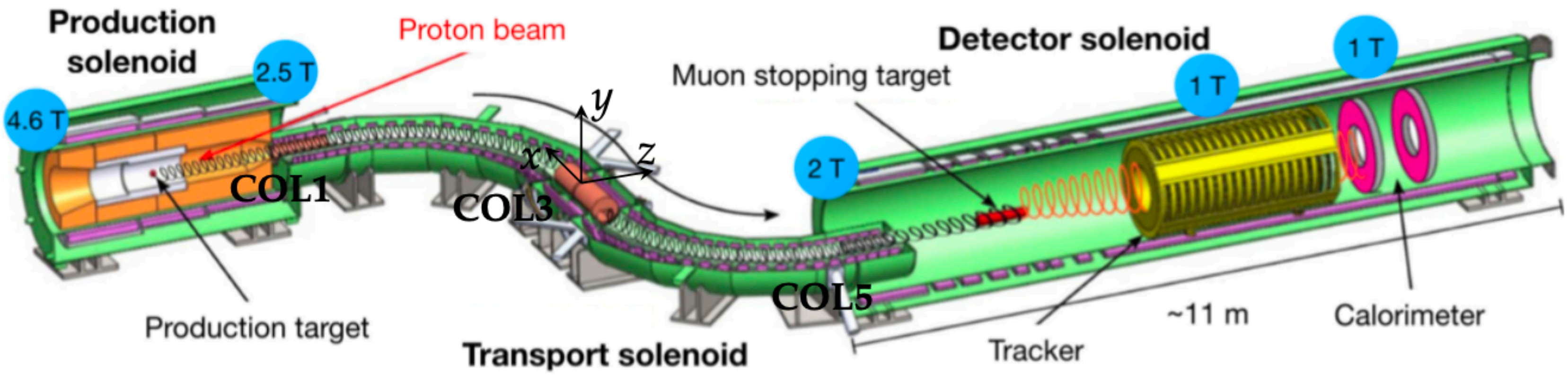

Production Solenoid

8 GeV pulsed proton beam interacts with the Tungsten target.

Mostly produces pions, decay into muons.

Transport Solenoid

“S” shape removes line of sight backgrounds.

Selects muons with $p < \sim 100 \mathrm{MeV/c}$.

Rotating collimator COL3 selects μ^- or μ^+ beam.

Mu2e Experimental Setup

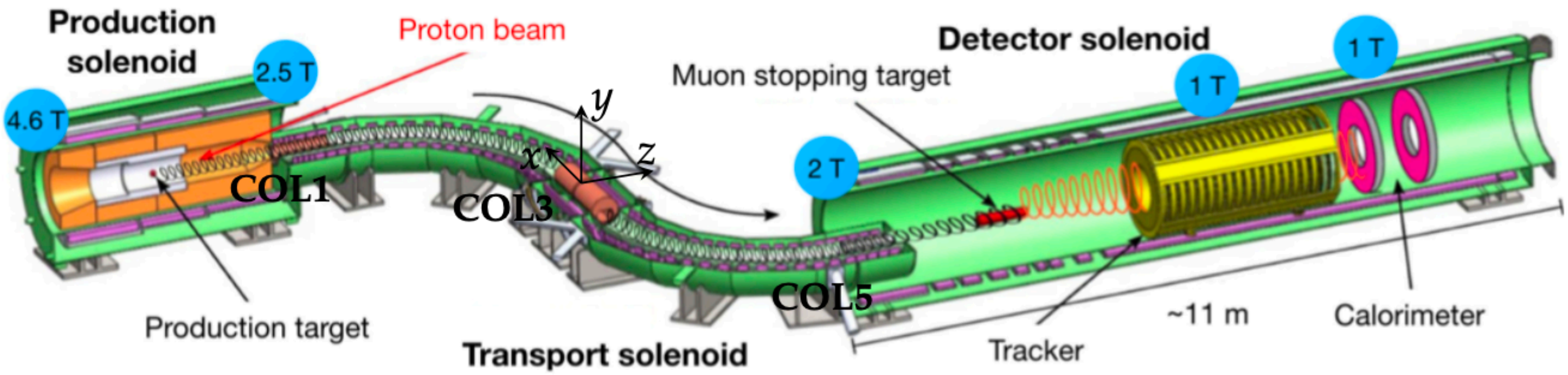

Production Solenoid

8 GeV pulsed proton beam interacts with the Tungsten target.

Mostly produces pions, decay into muons.

Transport Solenoid

"S" shape removes line of sight backgrounds.

Selects muons with $p < \sim 100 \mathrm{MeV/c}$.

Rotating collimator COL3 selects μ^- or μ^+ beam.

Detector Solenoid

Muons stop in the Al stopping target (ST).

Annular tracker and calorimeter to detect potential conversion e^-.

Mu2e: Proton delivery

Mu2e: Proton delivery

- Get 0.4 s of pulsed proton beam per 1.4 s Booster cycle.

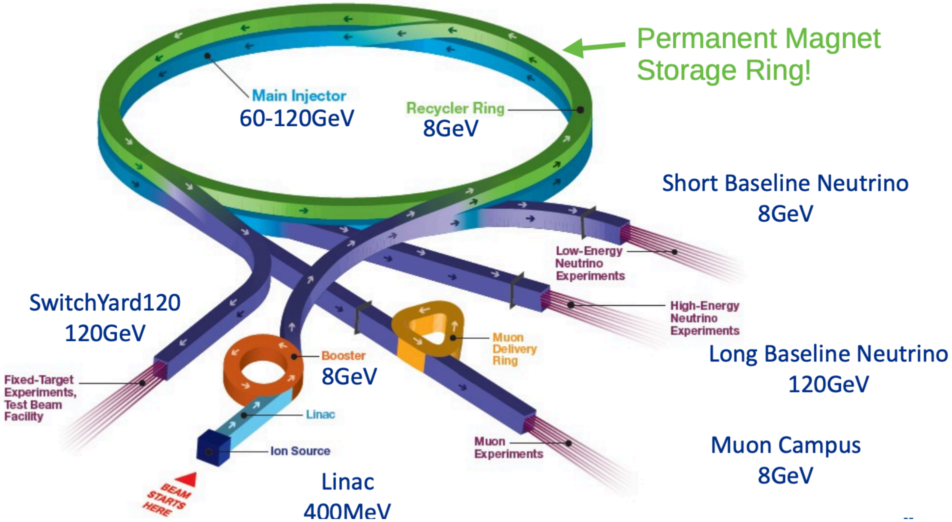

Mu2e: Proton delivery

- Get 0.4 s of pulsed proton beam per 1.4 s Booster cycle.

- Recycler ring - Delivery ring.

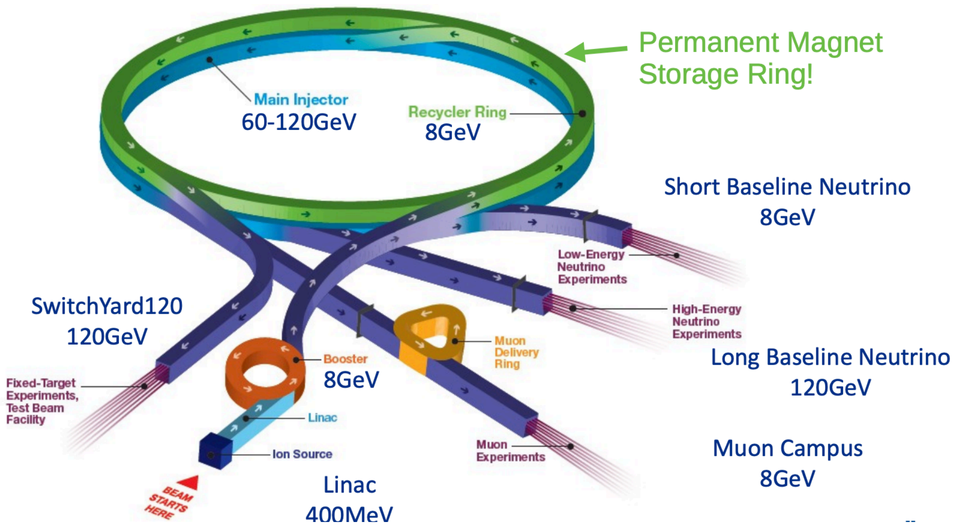

Mu2e: Proton delivery

- Get 0.4 s of pulsed proton beam per 1.4 s Booster cycle.
- Recycler ring - Delivery ring.
- Beam to Mu2e is resonantly slow extracted from the Delivery Ring.

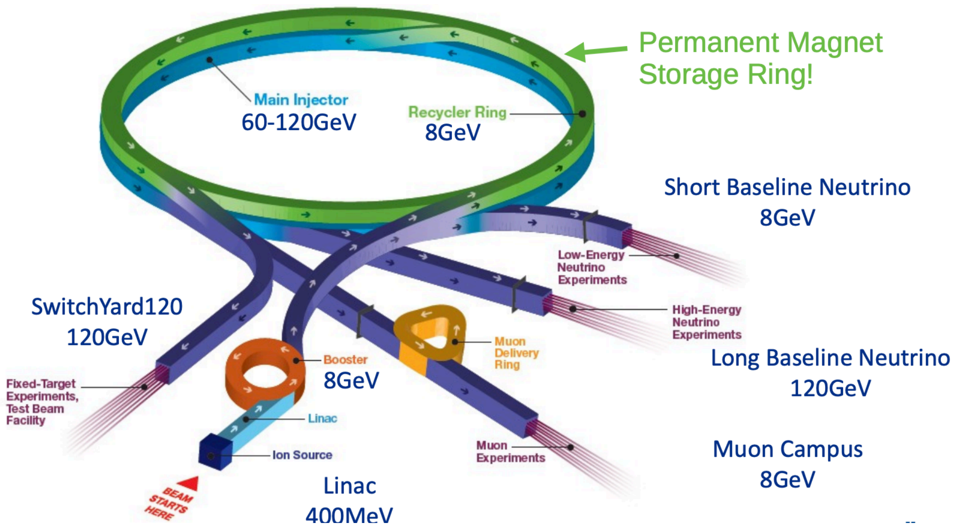

Mu2e: Proton delivery

- Get 0.4 s of pulsed proton beam per 1.4 s Booster cycle.
- Recycler ring - Delivery ring.
- Beam to Mu2e is resonantly slow extracted from the Delivery Ring.
- Peel off small fraction of stored beam every delivery ring orbital period = 1695 ns.

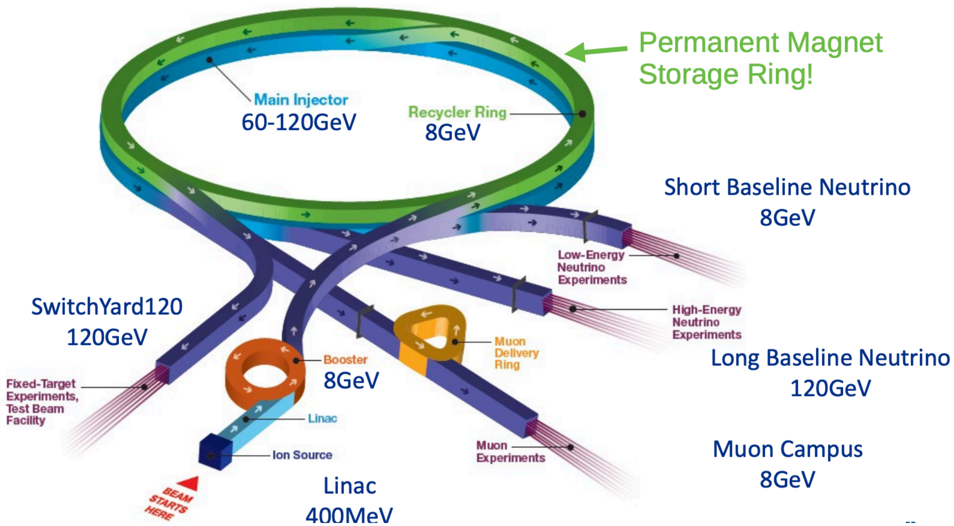

Mu2e: Proton delivery

- Get 0.4 s of pulsed proton beam per 1.4 s Booster cycle.
- Recycler ring - Delivery ring.
- Beam to Mu2e is resonantly slow extracted from the Delivery Ring.
- Peel off small fraction of stored beam every delivery ring orbital period = 1695 ns.
- Run 1 (2026 before LBNF/PIP-II shutdown) will use the Booster and current Linac.

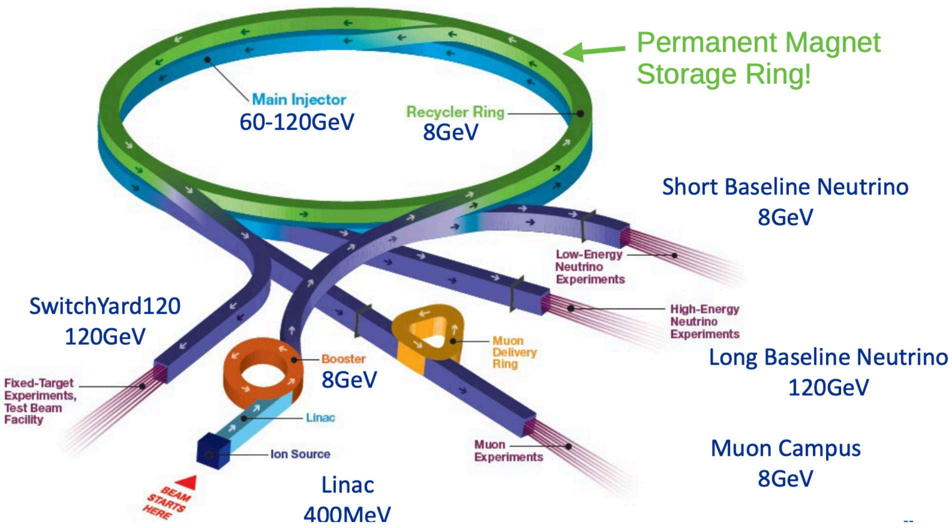

Mu2e: Proton delivery

- Get 0.4 s of pulsed proton beam per 1.4 s Booster cycle.
- Recycler ring - Delivery ring.
- Beam to Mu2e is resonantly slow extracted from the Delivery Ring.
- Peel off small fraction of stored beam every delivery ring orbital period = 1695 ns.
- Run 1 (2026 before LBNF/PIP-II shutdown) will use the Booster and current Linac.
- Run 2, after shutdown, use new PIP-II Linac to inject into Booster.

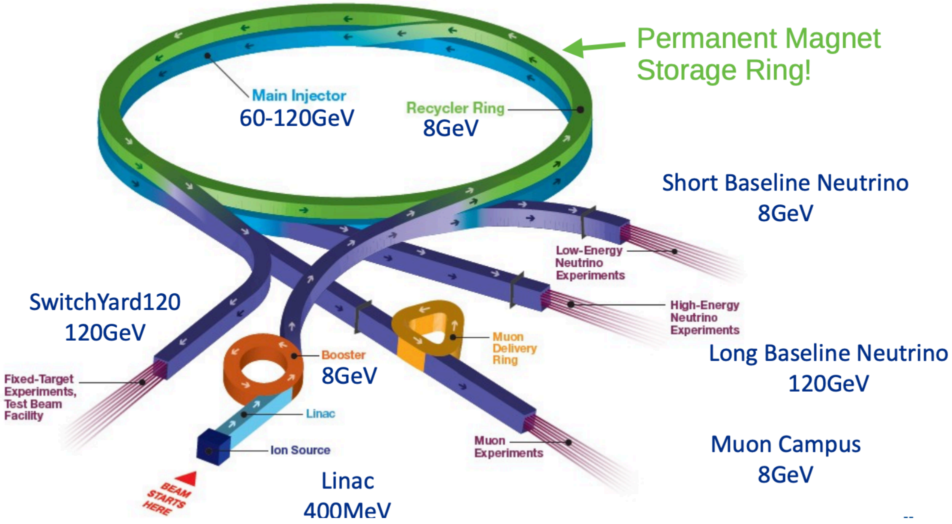

Mu2e Detectors

Straw Tracker

Mu2e Detectors

Straw Tracker

- Need a high-resolution momentum measurement.

Mu2e Detectors

Straw Tracker

- Need a high-resolution momentum measurement.

- Reduce low momentum background hits with the central hole.

Mu2e Detectors

Straw Tracker

- Need a high-resolution momentum measurement.
- Reduce low momentum background hits with the central hole.
- Made of mylar straw drift tubes, 96 straws per panel, 6 panels per plane, 2 planes per station, 18 stations in total.

Mu2e Detectors

Straw Tracker

- Need a high-resolution momentum measurement.
- Reduce low momentum background hits with the central hole.
- Made of mylar straw drift tubes, 96 straws per panel, 6 panels per plane, 2 planes per station, 18 stations in total.

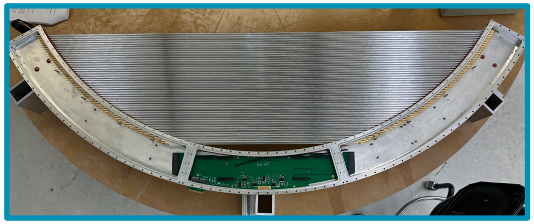

Mu2e Detectors

Straw Tracker

- Need a high-resolution momentum measurement.
- Reduce low momentum background hits with the central hole.
- Made of mylar straw drift tubes, 96 straws per panel, 6 panels per plane, 2 planes per station, 18 stations in total.

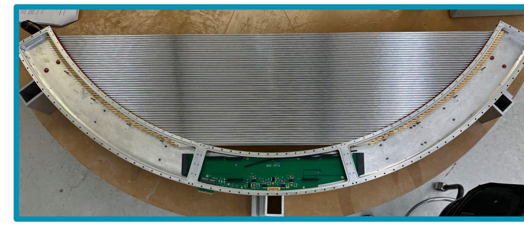

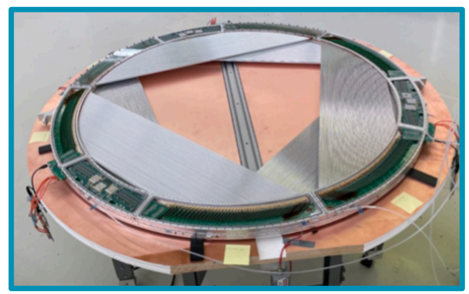

Mu2e Detectors

Straw Tracker

- Need a high-resolution momentum measurement.
- Reduce low momentum background hits with the central hole.
- Made of mylar straw drift tubes, 96 straws per panel, 6 panels per plane, 2 planes per station, 18 stations in total.

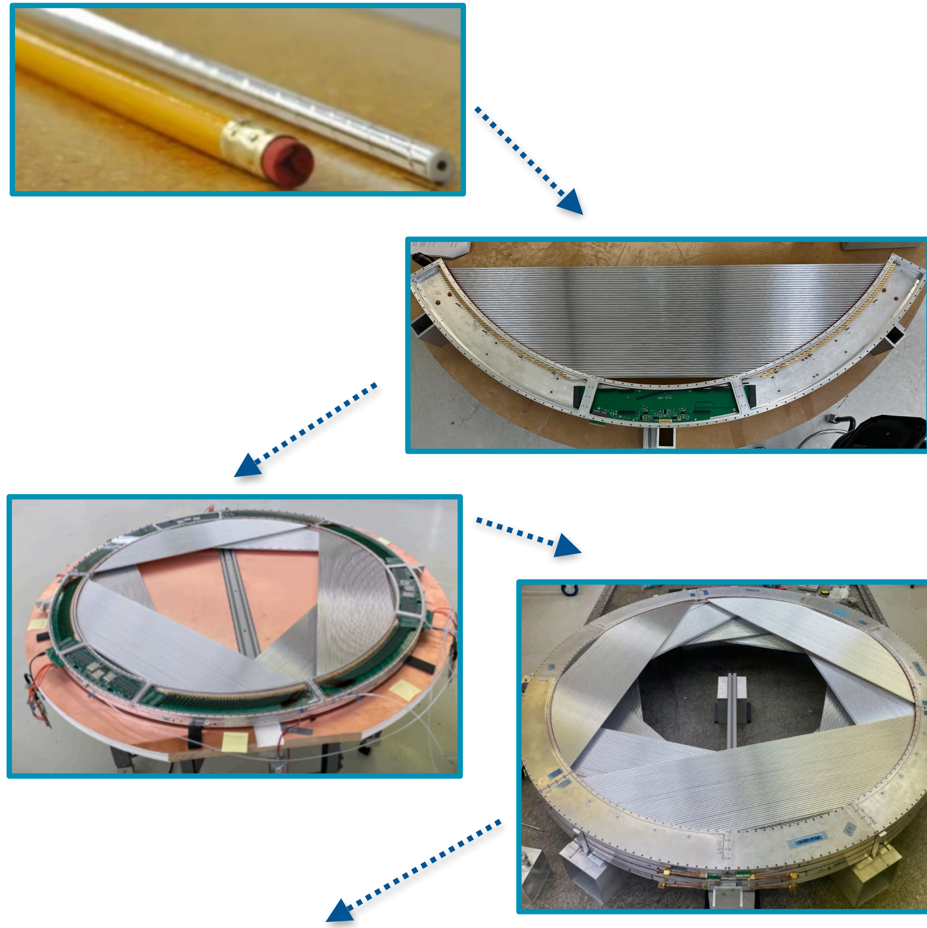

Mu2e Detectors

Straw Tracker

- Need a high-resolution momentum measurement.
- Reduce low momentum background hits with the central hole.
- Made of mylar straw drift tubes, 96 straws per panel, 6 panels per plane, 2 planes per station, 18 stations in total.

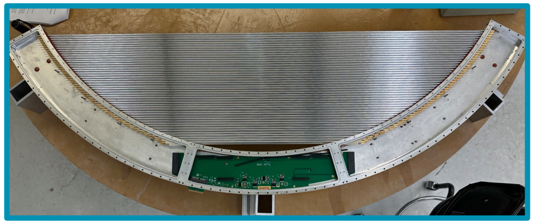

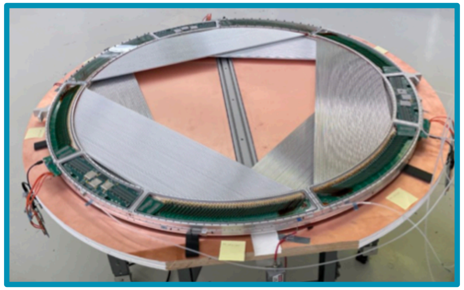

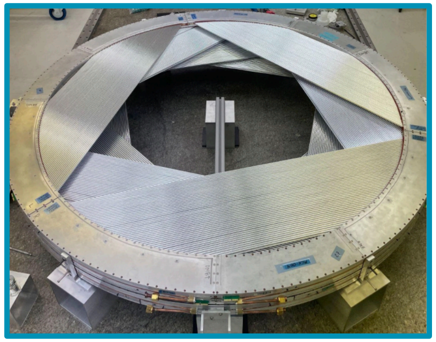

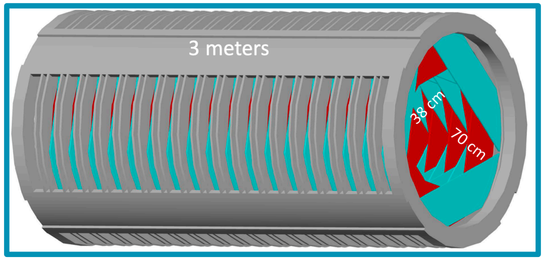

Mu2e Detectors

Straw Tracker

- Need a high-resolution momentum measurement.
- Reduce low momentum background hits with the central hole.
- Made of mylar straw drift tubes, 96 straws per panel, 6 panels per plane, 2 planes per station, 18 stations in total.
- Straws are filled with 80%:20% $Ar : CO_2$ mixture.

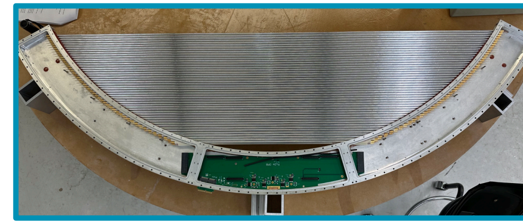

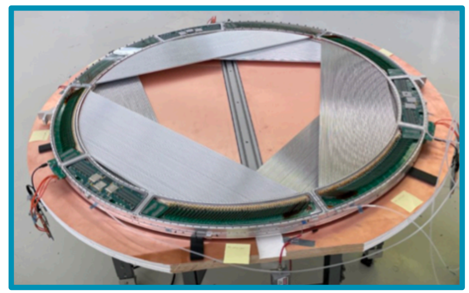

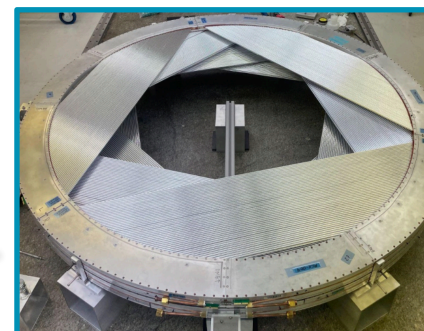

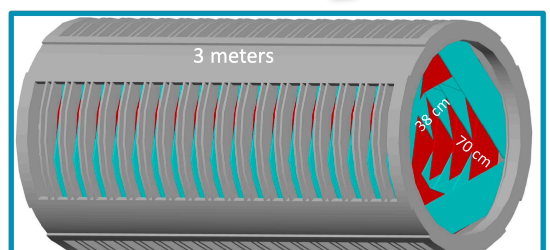

Mu2e Detectors

Straw Tracker

- Need a high-resolution momentum measurement.
- Reduce low momentum background hits with the central hole.
- Made of mylar straw drift tubes, 96 straws per panel, 6 panels per plane, 2 planes per station, 18 stations in total.
- Straws are filled with 80%:20% $Ar : CO_2$ mixture.
- For 100 MeV/c electrons, the intrinsic momentum resolution of the tracker is $\Delta p_{trk} < 300$ keV/c FWHM.

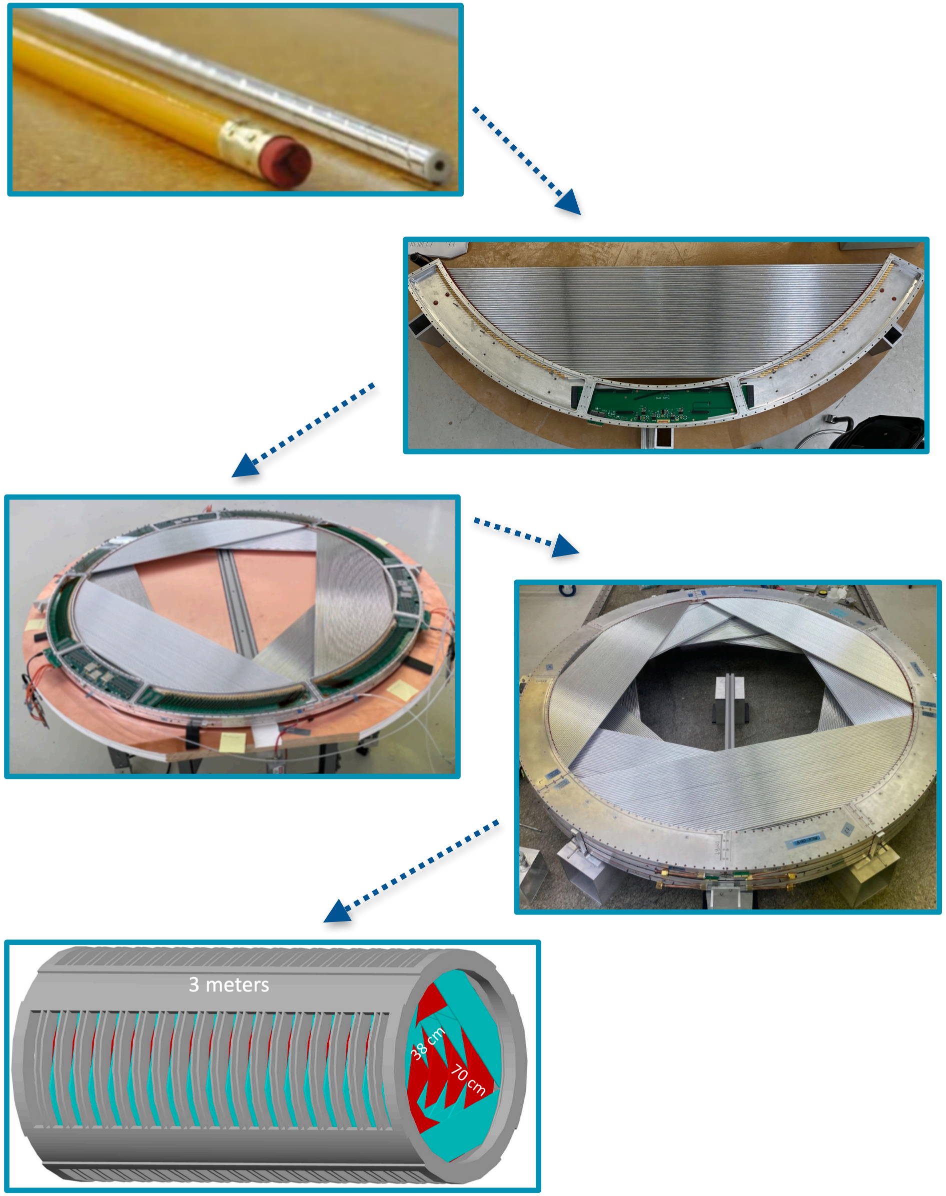

Mu2e Detectors

Electromagnetic Calorimeter

Mu2e Detectors

Electromagnetic Calorimeter

- 2 annular disks covering radii 37 cm - 66 cm. Each disk has 674 pure CsI crystals.

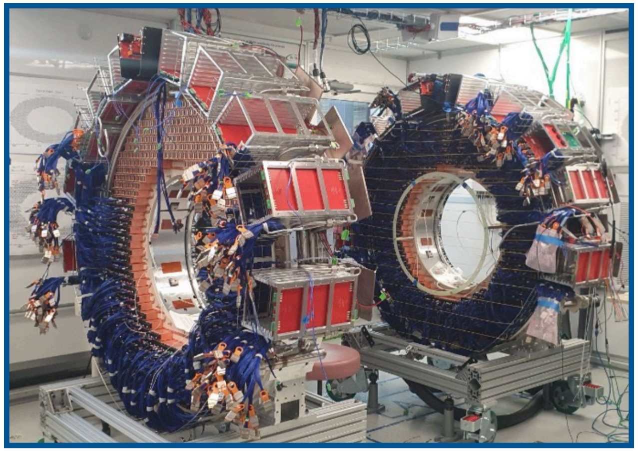

Mu2e Detectors

Electromagnetic Calorimeter

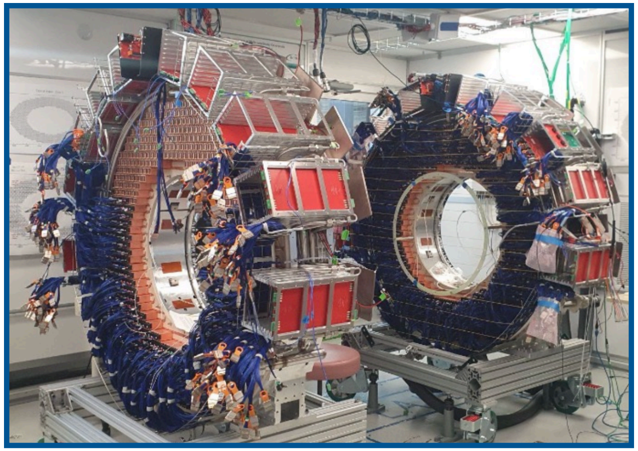

- 2 annular disks covering radii 37 cm - 66 cm. Each disk has 674 pure CsI crystals.

- For each crystal, two custom arrays large area UV-extended SiPMs for readout.

Mu2e Detectors

Electromagnetic Calorimeter

- 2 annular disks covering radii 37 cm - 66 cm. Each disk has 674 pure CsI crystals.

- For each crystal, two custom arrays large area UV-extended SiPMs for readout.

- Requirements for 100 MeV e^- at 50^o impact angle:
  -> $\sigma_E/E = O(10\%)$ for CE
  -> $\sigma_T = 500$ ps
  -> $\sigma_{X,Y} \leq 1$cm

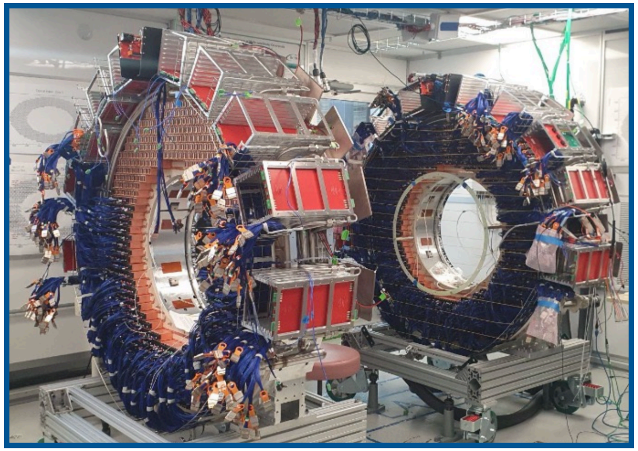

Mu2e Detectors

Electromagnetic Calorimeter

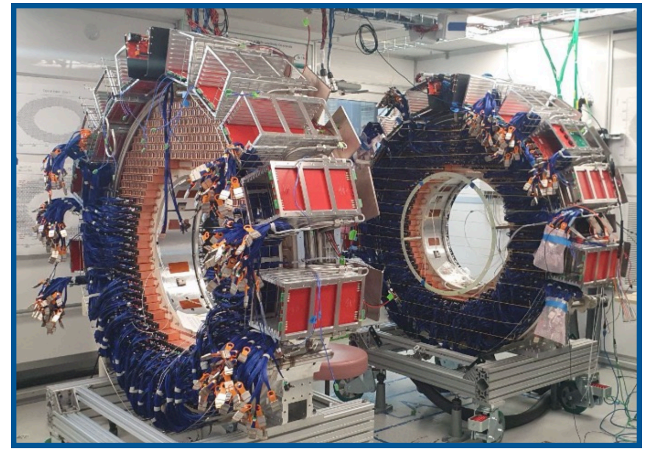

- 2 annular disks covering radii 37 cm - 66 cm. Each disk has 674 pure CsI crystals.

- For each crystal, two custom arrays large area UV-extended SiPMs for readout.

- Requirements for 100 MeV e^- at 50^o impact angle:
  -> $\sigma_E/E = O(10\%)$ for CE
  -> $\sigma_T = 500$ ps
  -> $\sigma_{X,Y} \leq 1$cm

- Test beam results for 100 MeV e- beam give energy resolution of 16.4% FWHM and timing resolution of 110 ps*.

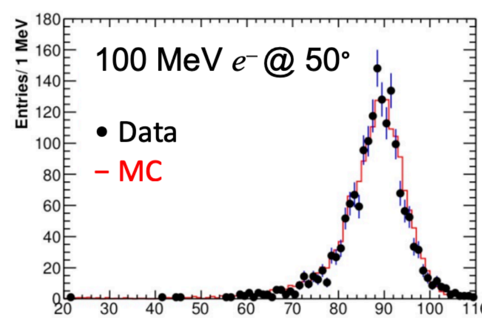

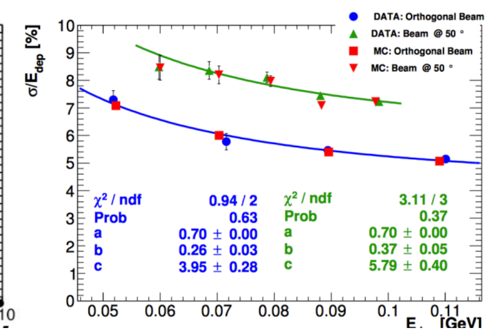

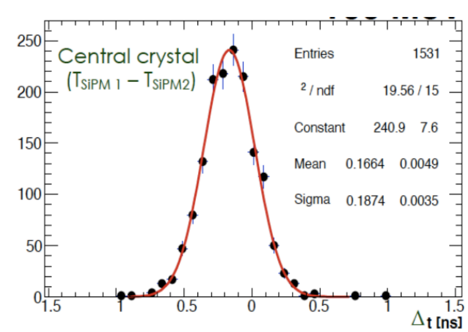

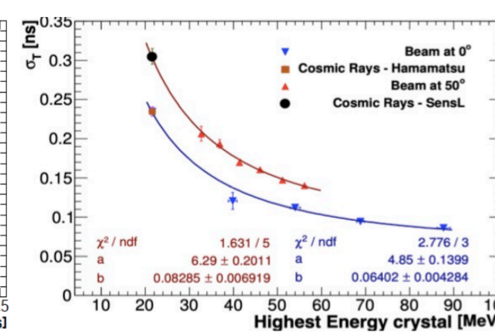

https://doi.org/10.1016/j.nima.2019.04.094

Mu2e Detectors

Cosmic Ray Veto

Mu2e Detectors

Cosmic Ray Veto

- Layers of polystyrene scintillator counters with embedded wavelength-shifting fibres, read out with silicon photomultipliers (SiPMs).

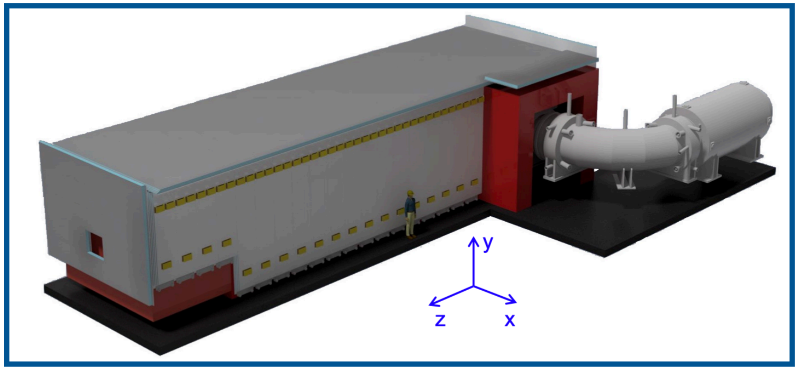

Mu2e Detectors

Cosmic Ray Veto

- Layers of polystyrene scintillator counters with embedded wavelength-shifting fibres, read out with silicon photomultipliers (SiPMs).

- Encloses the detector solenoid and half of the transport solenoid.

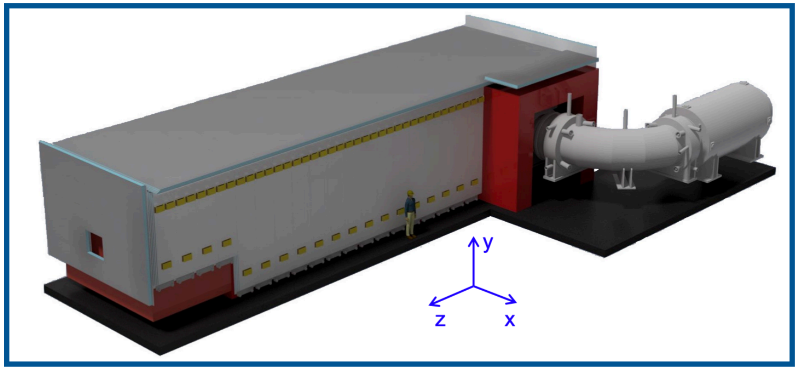

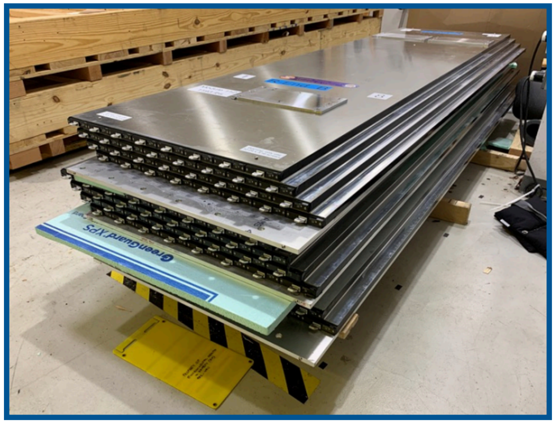

Mu2e Detectors

Cosmic Ray Veto

- Layers of polystyrene scintillator counters with embedded wavelength-shifting fibres, read out with silicon photomultipliers (SiPMs).
- Encloses the detector solenoid and half of the transport solenoid.
- CRV "track stub", or coincidence, is typically defined as a minimum of 3/4 layers hit, above some photoelectron threshold, localised in time and space.

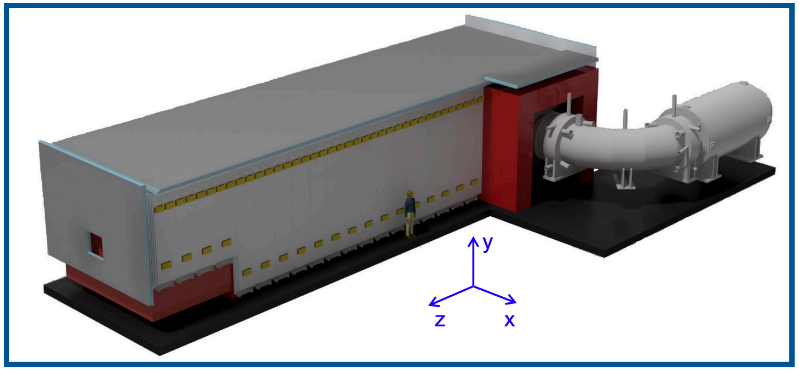

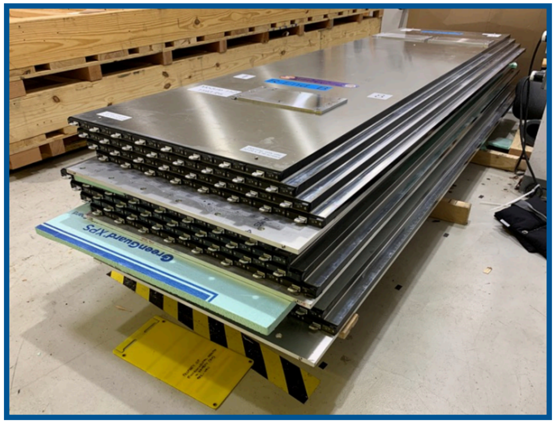

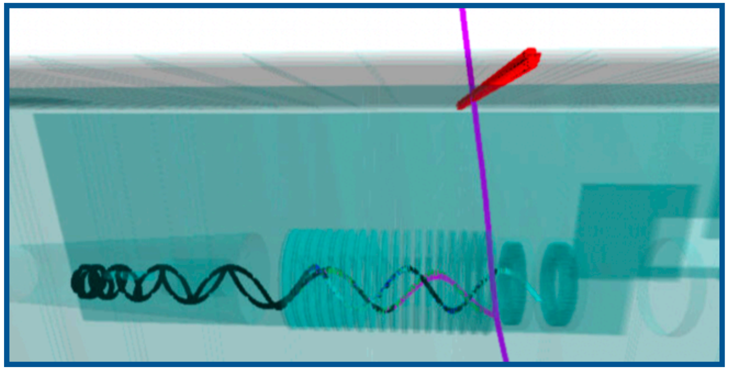

Mu2e Detectors

Cosmic Ray Veto

- Layers of polystyrene scintillator counters with embedded wavelength-shifting fibres, read out with silicon photomultipliers (SiPMs).
- Encloses the detector solenoid and half of the transport solenoid.
- CRV "track stub", or coincidence, is typically defined as a minimum of 3/4 layers hit, above some photoelectron threshold, localised in time and space.
- Mu2e sensitivity requirements require the CRV to possess an overall efficiency of 99.99%.

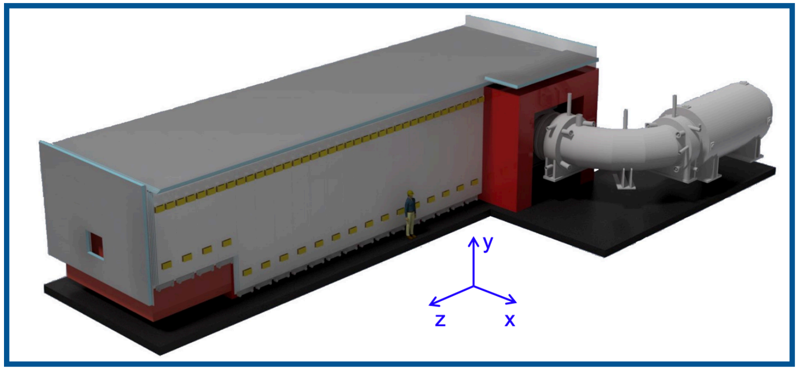

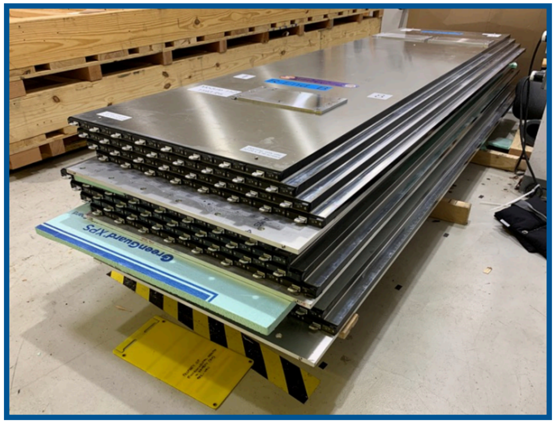

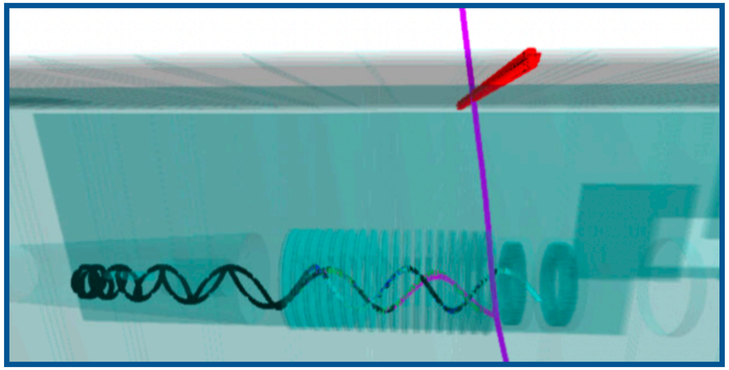

Mu2e Detectors

Stopping Target Monitor

Mu2e Detectors

Stopping Target Monitor

- STM is the primary means of normalisation for Mu2e.

$$R_{\mu e} = \frac{\Gamma(\mu^- + N(Z,A) \rightarrow e^- + N(Z,A))}{\Gamma(\mu^- + N(Z,A) \rightarrow \nu_\mu + N(Z-1,A))}$$

Mu2e Detectors

Stopping Target Monitor

- STM is the primary means of normalisation for Mu2e.

$$R_{\mu e} = \frac{\Gamma(\mu^- + N(Z,A) \rightarrow e^- + N(Z,A))}{\boxed{\Gamma(\mu^- + N(Z,A) \rightarrow \nu_\mu + N(Z-1,A))}}$$

Mu2e Detectors

Stopping Target Monitor

- STM is the primary means of normalisation for Mu2e.
- Composed of HPGe and LaBr detectors.

$$R_{\mu e} = \frac{\Gamma(\mu^- + N(Z,A) \rightarrow e^- + N(Z,A))}{\boxed{\Gamma(\mu^- + N(Z,A) \rightarrow \nu_\mu + N(Z-1,A))}}$$

Mu2e Detectors

Stopping Target Monitor

- STM is the primary means of normalisation for Mu2e.
- Composed of HPGe and LaBr detectors.
- Measures rates of low energy secondary photons emitted from the target due to muon interactions.

$$R_{\mu e} = \frac{\Gamma(\mu^- + N(Z,A) \to e^- + N(Z,A))}{\boxed{\Gamma(\mu^- + N(Z,A) \to \nu_\mu + N(Z-1,A))}}$$

Mu2e Detectors

Stopping Target Monitor

- STM is the primary means of normalisation for Mu2e.
- Composed of HPGe and LaBr detectors.
- Measures rates of low energy secondary photons emitted from the target due to muon interactions.
- For Al target, use at least one of the transitions:

  -> Muonic 2p-1s X-ray at 347 keV, emitted promptly when muon stops (78% BR, 200-400 ns after proton pulse).
  -> Gamma ray at 1809 keV emitted promptly when muon captures on the Al nucleus (~30% BR,with 864 ns lifetime of muon Al).
  -> Gamma ray at 844 keV emitted during the beta decay of daughter nucleus (~8% BR, 9.5 minute half-life, activated nucleus produced by muon capture).

$$R_{\mu e} = \frac{\Gamma(\mu^- + N(Z,A) \to e^- + N(Z,A))}{\boxed{\Gamma(\mu^- + N(Z,A) \to \nu_\mu + N(Z-1,A))}}$$

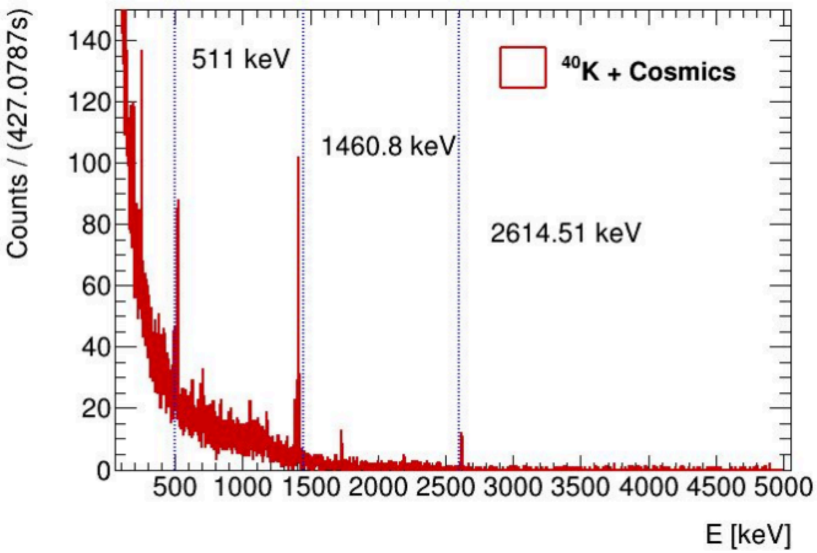

Background processes to $\mu^- \to e^-$ search

Decay in Orbit

Background processes to $\mu^- \rightarrow e^-$ search

Decay in Orbit

- In free μ^-decay, e^- kinematic endpoint is $m_\mu/2$ and follows Michel spectrum.

$$R = \frac{p\perp}{qB} = 35 \text{ cm}$$

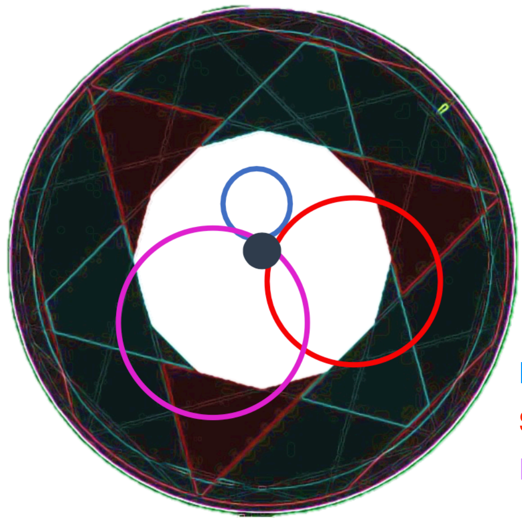

Michel e^- (< 52 MeV/c)
Signal (105 MeV/c)
Problematic DIO tail (> 100 MeV/c)

Background processes to $\mu^- \rightarrow e^-$ search

Decay in Orbit

- In free μ^-decay, e^- kinematic endpoint is $m_\mu/2$ and follows Michel spectrum.

$$R = \frac{p\perp}{qB} = 35 \text{ cm}$$

- In the field of a nucleus, μ^- decay endpoint is extended to the signal energy (105 MeV/c).

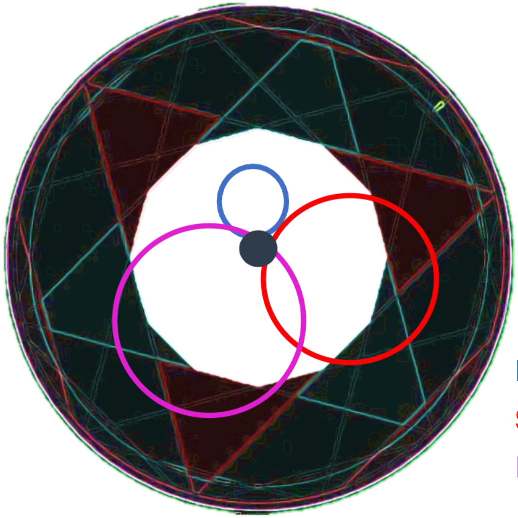

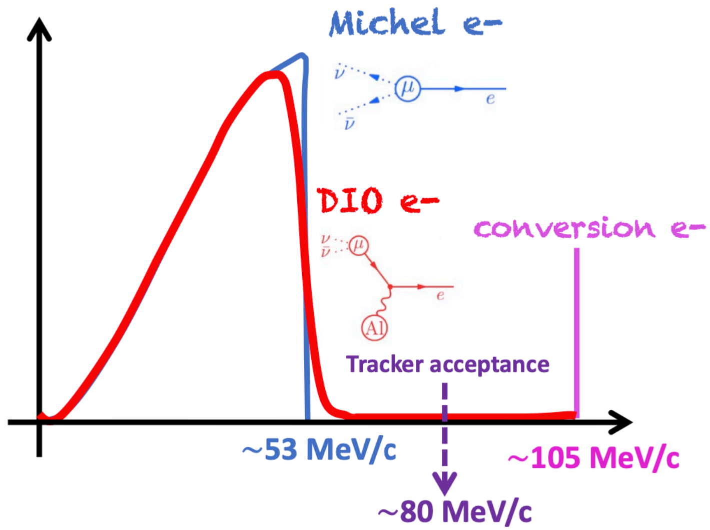

Background processes to $\mu^- \to e^-$ search

Decay in Orbit

- In free μ^-decay, e^- kinematic endpoint is $m_\mu/2$ and follows Michel spectrum.

$$R = \frac{p\perp}{qB} = 35 \text{ cm}$$

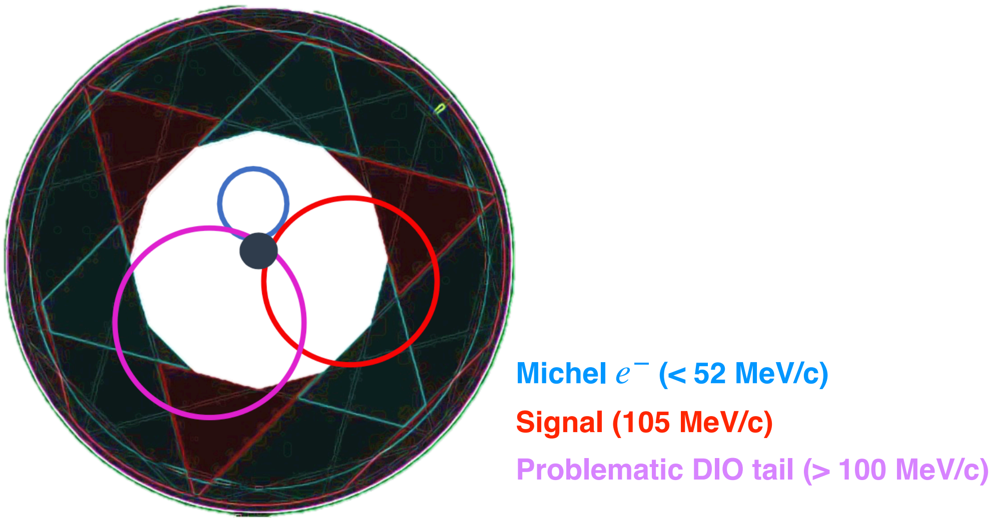

- In the field of a nucleus, μ^- decay endpoint is extended to the signal energy (105 MeV/c).

- Need a straw tracker with good momentum resolution, < 200 keV/c to distinguish DIO tail from signal.

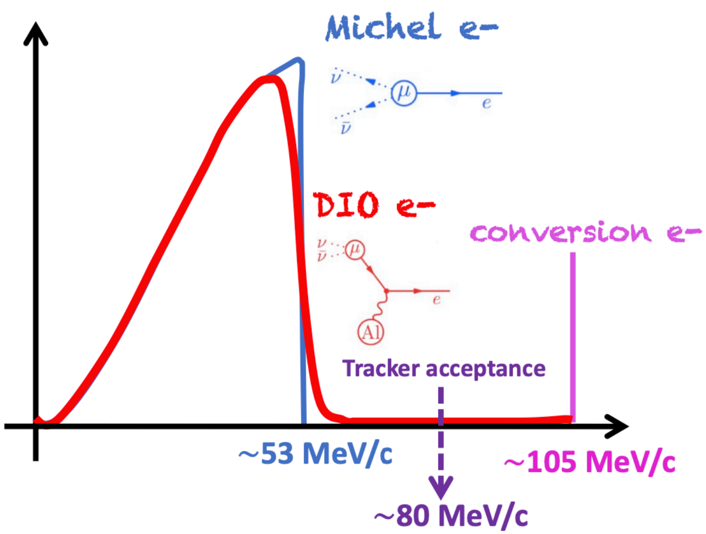

Background processes to $\mu^- \to e^-$ search

Cosmic rays

Background processes to $\mu^- \to e^-$ search

Cosmic rays

- Cosmic rays interacting with the detector material can produce signal-like e^-/e^+.

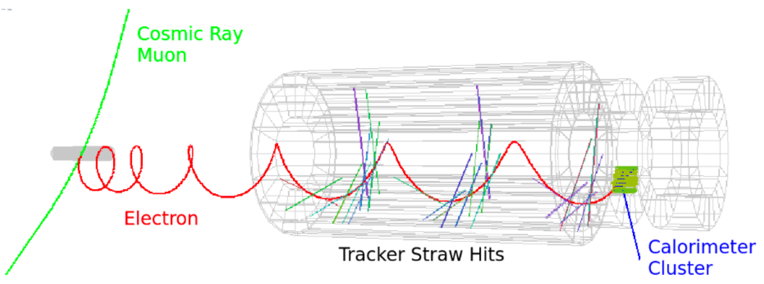

Background processes to $\mu^- \to e^-$ search

Cosmic rays

- Cosmic rays interacting with the detector material can produce signal-like e^-/e^+.

- We expect ~1 signal-like event per day.

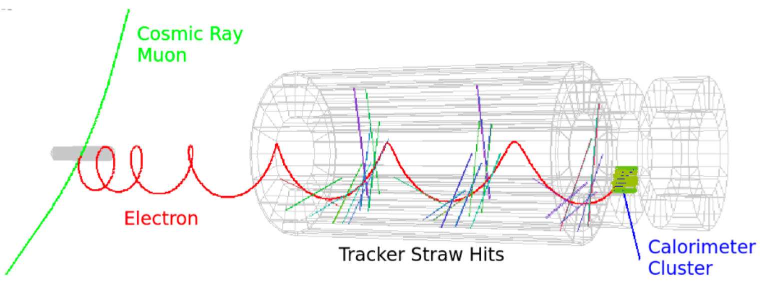

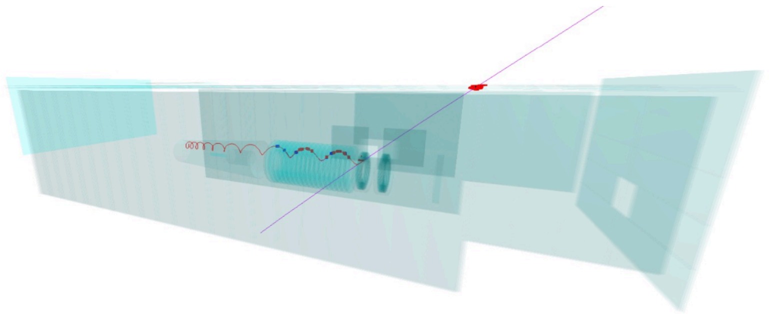

Background processes to $\mu^- \rightarrow e^-$ search

Cosmic rays

- Cosmic rays interacting with the detector material can produce signal-like e^-/e^+.
- We expect ~1 signal-like event per day.
- Cosmic ray events are identified by having a coincidence cluster in the CRV with hits in 3/4 layers.

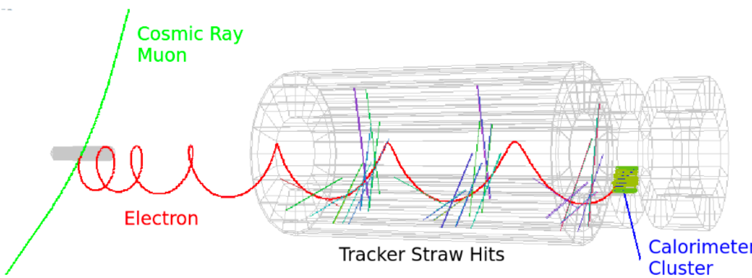

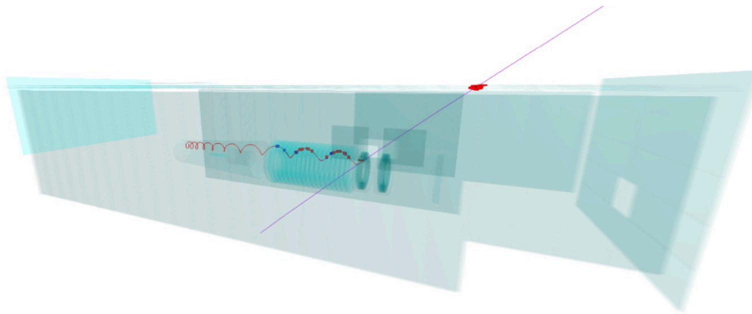

Background processes to $\mu^- \rightarrow e^-$ search

Cosmic rays

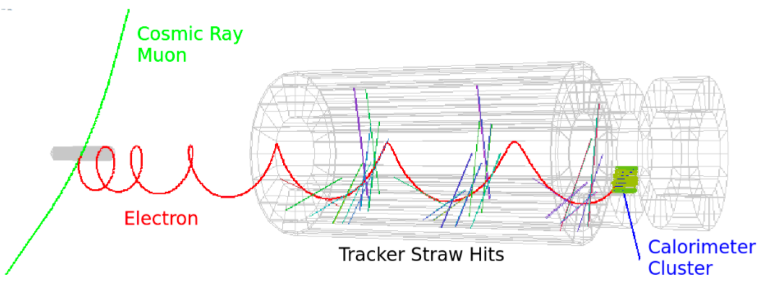

- Cosmic rays interacting with the detector material can produce signal-like e^-/e^+.

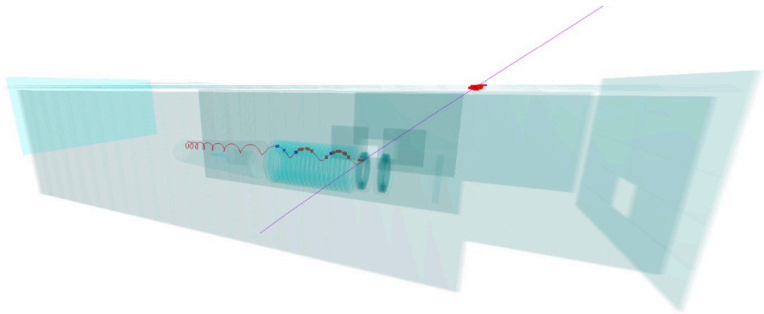

- We expect ~1 signal-like event per day.

- Cosmic ray events are identified by having a coincidence cluster in the CRV with hits in 3/4 layers.

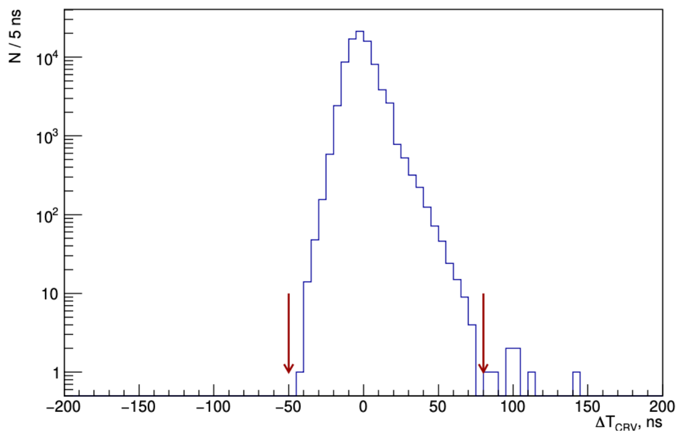

- The time of the reconstructed track matched to the CRV cluster is required to be within $-50 < t_{CRV} < 80$ ns of the cluster time.

Background processes to $\mu^- \to e^-$ search

Radiative Pion Capture

Background processes to $\mu^- \to e^-$ search

Radiative Pion Capture

- Pions contaminating the beam can survive to the stopping target, where radiative pion captures can produce signal-like e^-/e^+.

$\pi^- + N(A,Z) \to \gamma^{(*)} + N(A,Z-1)$ followed by $\gamma^{(*)} \to e^+ + e^-$.

Background processes to $\mu^- \to e^-$ search

Radiative Pion Capture

- Pions contaminating the beam can survive to the stopping target, where radiative pion captures can produce signal-like e^-/e^+.

$$\pi^- + N(A,Z) \to \gamma^{(*)} + N(A,Z-1) \text{ followed by } \gamma^{(*)} \to e^+ + e^-.$$

- Pion lifetime 26 ns at rest. Pulsed proton beam (250 ns wide, pulses are 1695 ns apart). We can wait out the pion decay.

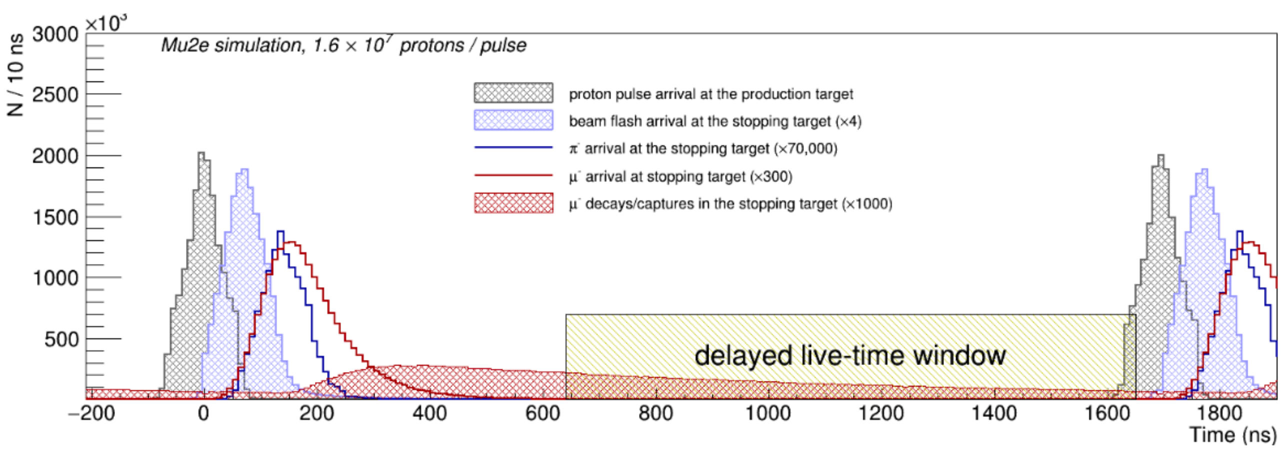

Background processes to $\mu^- \to e^-$ search

Radiative Pion Capture

- Pions contaminating the beam can survive to the stopping target, where radiative pion captures can produce signal-like e^-/e^+.

$$\pi^- + N(A,Z) \to \gamma^{(*)} + N(A,Z-1) \text{ followed by } \gamma^{(*)} \to e^+ + e^-.$$

- Pion lifetime 26 ns at rest. Pulsed proton beam (250 ns wide, pulses are 1695 ns apart). We can wait out the pion decay.

- In addition, upstream extinction removes out-of-time protons.

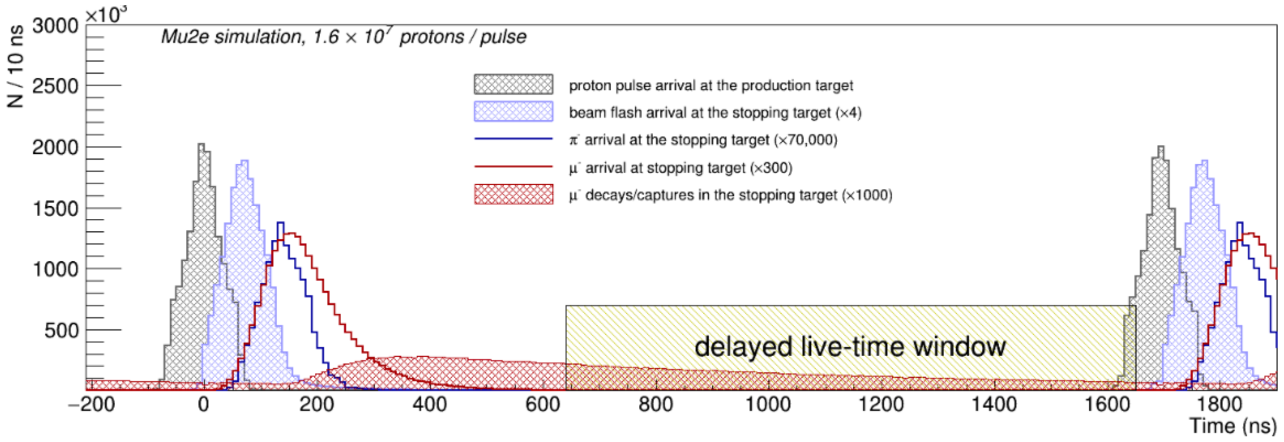

Background processes to $\mu^- \to e^-$ search

Antiprotons

Background processes to $\mu^- \to e^-$ search

Antiprotons

- $\overline{p}$s are produced by the pW interactions in the Production Solenoid.

Background processes to $\mu^- \to e^-$ search

Antiprotons

- $\overline{p}$s are produced by the pW interactions in the Production Solenoid.
- Relatively low background but high systematic uncertainty.

Background processes to $\mu^- \rightarrow e^-$ search

Antiprotons

- $\overline{p}$s are produced by the pW interactions in the Production Solenoid.
- Relatively low background but high systematic uncertainty.
- $p\overline{p}$ annihilation at ST can produce e^-s by $\pi^0 \rightarrow \gamma\gamma$ decays followed by the photon conversions and $\pi^- \rightarrow \mu^-\overline{\nu}$ decays followed by the μ^- decays.

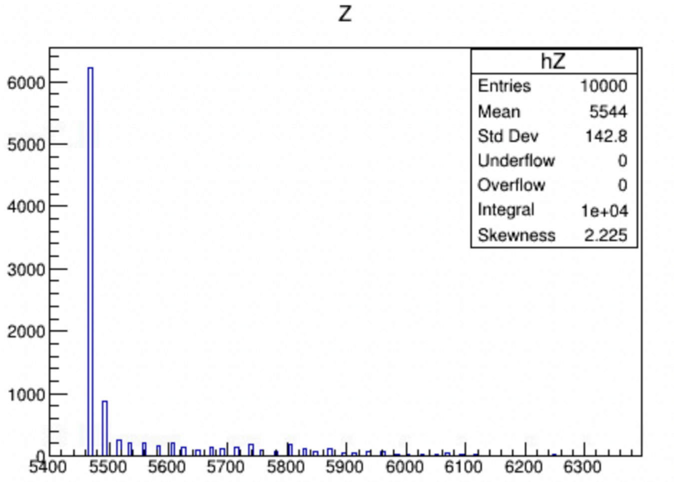

z (mm) from the centre of the TS
Longitudinal position of $\overline{p}$ annihilations

Background processes to $\mu^- \to e^-$ search

Antiprotons

- $\overline{p}$s are produced by the pW interactions in the Production Solenoid.
- Relatively low background but high systematic uncertainty.
- $p\overline{p}$ annihilation at ST can produce e^-s by $\pi^0 \to \gamma\gamma$ decays followed by the photon conversions and $\pi^- \to \mu^- \overline{\nu}$ decays followed by the μ^- decays.
- Can also cause delayed RPC.

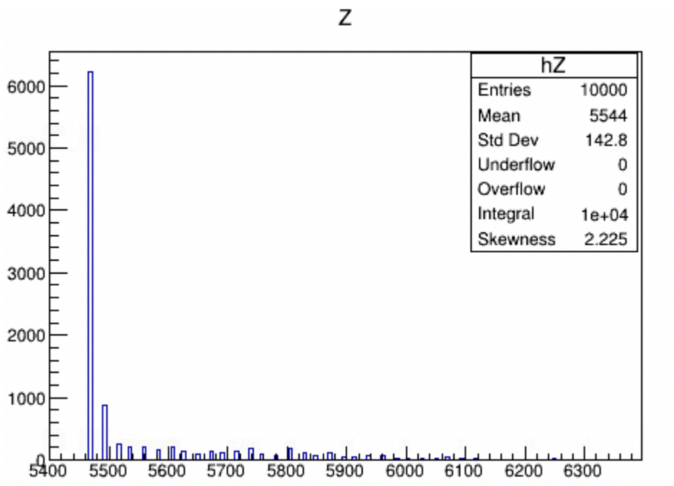

z (mm) from the centre of the TS
Longitudinal position of $\overline{p}$ annihilations

Background processes to $\mu^- \rightarrow e^-$ search

Antiprotons

- $\overline{p}$s are produced by the pW interactions in the Production Solenoid.
- Relatively low background but high systematic uncertainty.
- $p\overline{p}$ annihilation at ST can produce e^-s by $\pi^0 \rightarrow \gamma\gamma$ decays followed by the photon conversions and $\pi^- \rightarrow \mu^-\overline{\nu}$ decays followed by the μ^- decays.
- Can also cause delayed RPC.
- Background induced by $\overline{p}$ cannot be efficiently suppressed by time window cut used to reduce prompt background.

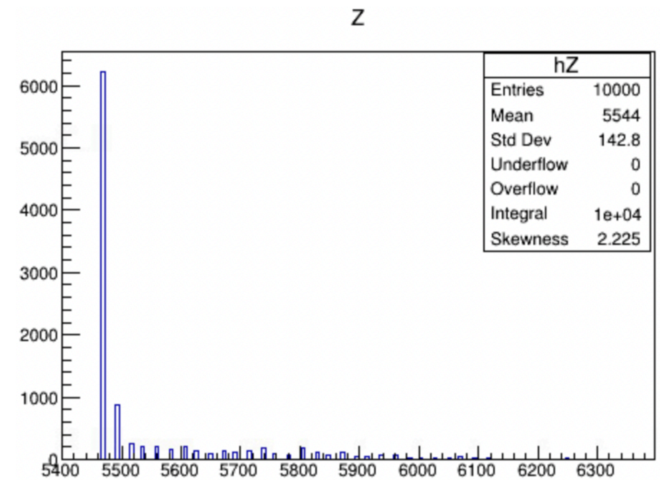

z (mm) from the centre of the TS
Longitudinal position of $\overline{p}$ annihilations

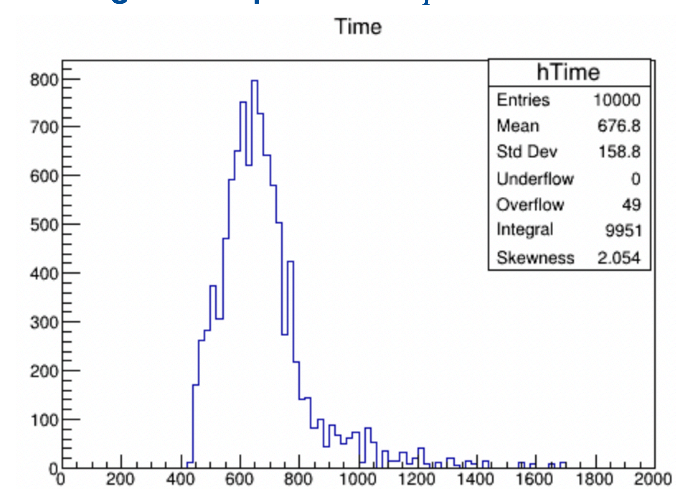

time (ns) of $\overline{p}$ annihilations
$\overline{p}$s stop within the live data taking window

Background processes to $\mu^- \to e^-$ search

Antiprotons

- $\overline{p}$s are produced by the pW interactions in the Production Solenoid.
- Relatively low background but high systematic uncertainty.
- $p\overline{p}$ annihilation at ST can produce e^-s by $\pi^0 \to \gamma\gamma$ decays followed by the photon conversions and $\pi^- \to \mu^-\overline{\nu}$ decays followed by the μ^- decays.
- Can also cause delayed RPC.
- Background induced by $\overline{p}$ cannot be efficiently suppressed by time window cut used to reduce prompt background.
- Absorber elements at entrance and centre of the Transport Solenoid to suppress the $\overline{p}$ background.

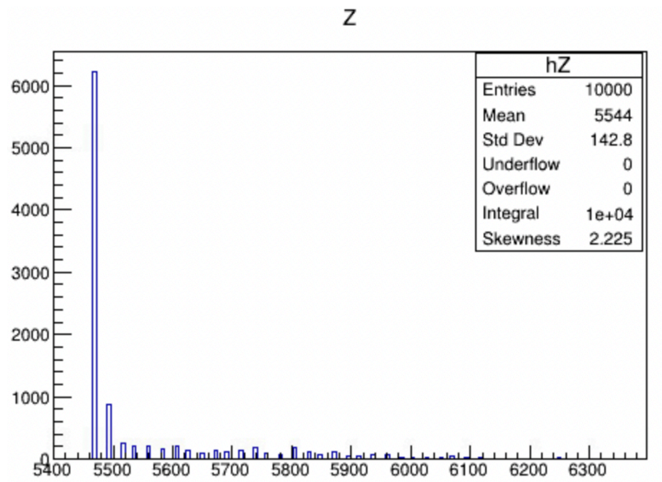

z (mm) from the centre of the TS
Longitudinal position of $\overline{p}$ annihilations

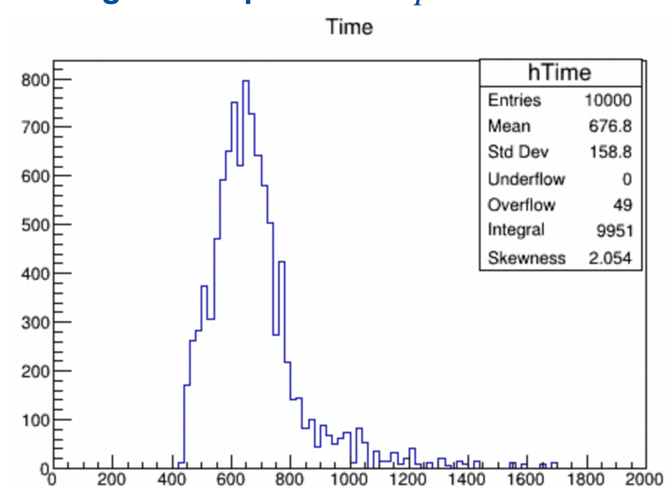

time (ns) of $\overline{p}$ annihilations
$\overline{p}$s stop within the live data taking window

Background summary

Channel	Mu2e Run I
Cosmic rays	$0.046 \pm 0.010(stat) \pm 0.009(syst)$
Decay in Orbit	$0.038 \pm 0.002(stat)^{+0.025}_{-0.015}(syst)$
Antiprotons	$0.010 \pm 0.003(stat) \pm 0.010(syst)$
RPC in-time	$0.010 \pm 0.002(stat)^{+0.001}_{-0.003}(syst)$
RPC out-of-time	$(1.2 \pm 0.1(stat)^{+0.1}_{-0.3}(syst)) \times 10^{-3}$
Radiative Muon Capture	$< 2.4 \times 10^{-3}$
Decays in flight	$< 2 \times 10^{-3}$
Beam electrons	$< 1 \times 10^{-3}$
Total	0.105 ± 0.032

Background summary using the optimised signal momentum and time window 103.6<p<104.90 MeV/c and 640< T0<1650 ns*

*Mu2e Collaboration MDPI Universe 2023 https://doi.org/10.3390/universe9010054

Expected sensitivity

Expected sensitivity

Expected sensitivity

- Mu2e Run I assumes an integrated flux of 6×10^{16} muons.

*Mu2e Collaboration MDPI Universe 2023 https://doi.org/10.3390/universe9010054

Expected sensitivity

- Mu2e Run I assumes an integrated flux of 6×10^{16} muons.

- The optimised signal window if $t0 \in [640,1650]$ ns and $p \in [10.6,104.9]$ MeV/c.

*Mu2e Collaboration MDPI Universe 2023 https://doi.org/10.3390/universe9010054

Expected sensitivity

- Mu2e Run I assumes an integrated flux of 6×10^{16} muons.

- The optimised signal window if $t0 \in [640{,}1650]$ ns and $p \in [10.6{,}104.9]$ MeV/c.

- Single-Event-Sensitivity of 2.3×10^{-16} and a total signal selection efficiency of 11.7%.

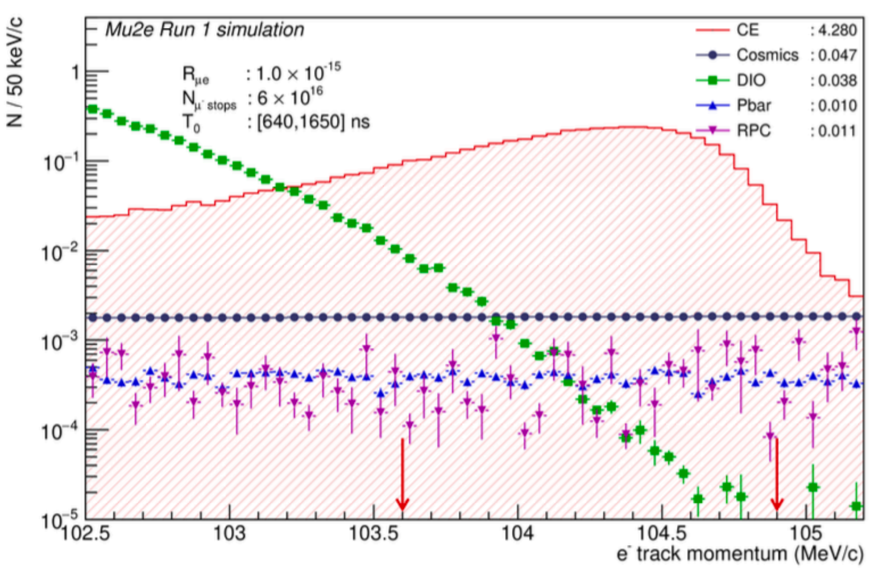

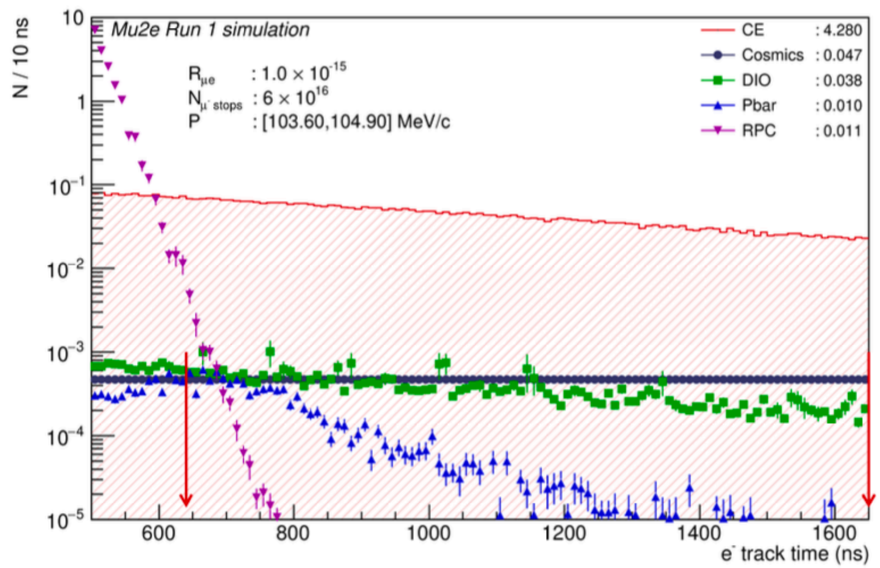

*Mu2e Collaboration MDPI Universe 2023 https://doi.org/10.3390/universe9010054

Expected sensitivity

- Mu2e Run I assumes an integrated flux of 6×10^{16} muons.
- The optimised signal window if $t0 \in [640,1650]$ ns and $p \in [10.6,104.9]$ MeV/c.
- Single-Event-Sensitivity of 2.3×10^{-16} and a total signal selection efficiency of 11.7%.
- The expected Run I 5σ discovery sensitivity is $R_{\mu e} = 1.2 \times 10^{-15}$.

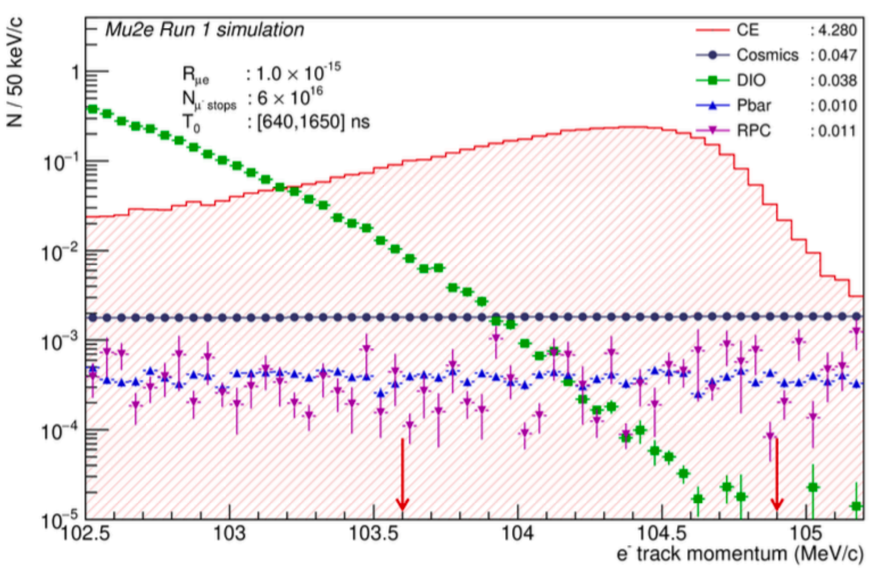

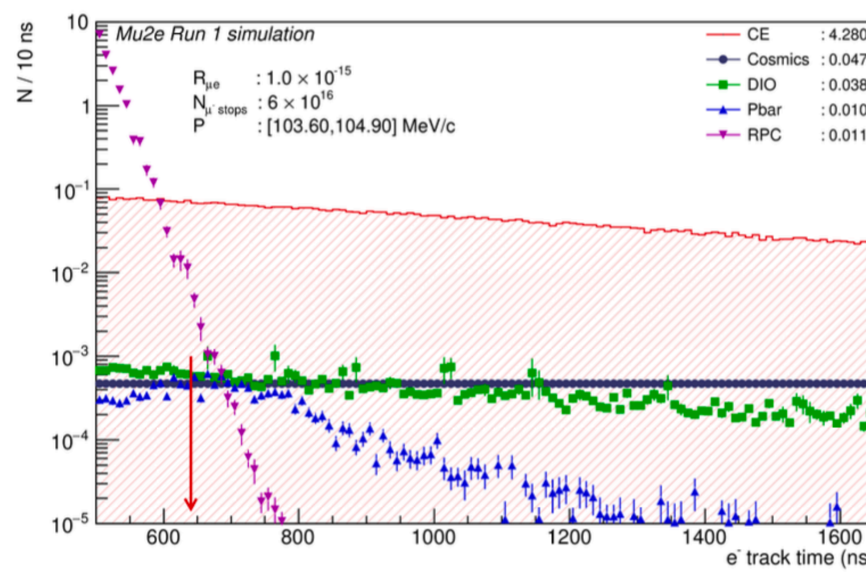

*Mu2e Collaboration MDPI Universe 2023 https://doi.org/10.3390/universe9010054

Expected sensitivity

- Mu2e Run I assumes an integrated flux of 6×10^{16} muons.
- The optimised signal window if $t0 \in [640{,}1650]$ ns and $p \in [10.6{,}104.9]$ MeV/c.
- Single-Event-Sensitivity of 2.3×10^{-16} and a total signal selection efficiency of 11.7%.
- The expected Run I 5σ discovery sensitivity is $R_{\mu e} = 1.2 \times 10^{-15}$.
- If no signal, the expected upper limit is $R_{\mu e} < 6.2 \times 10^{-16}$ at 90% CL.

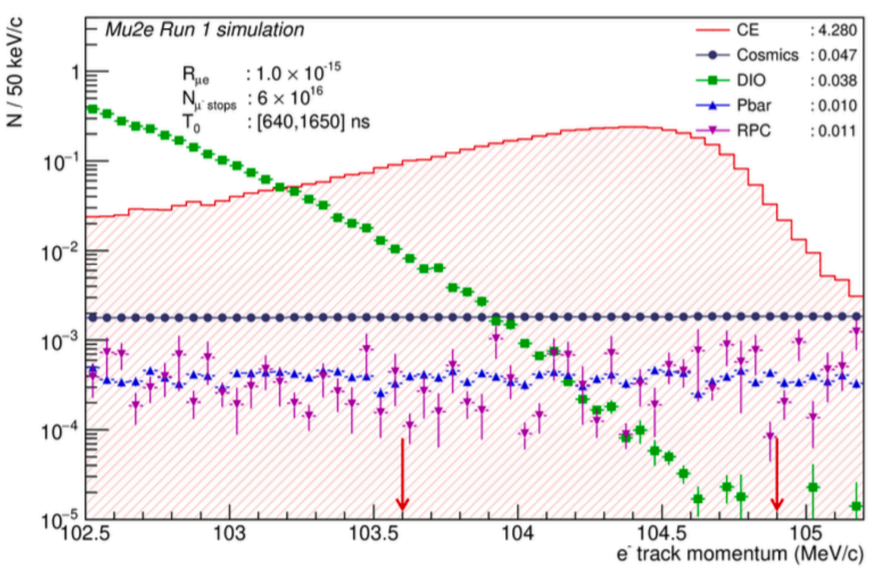

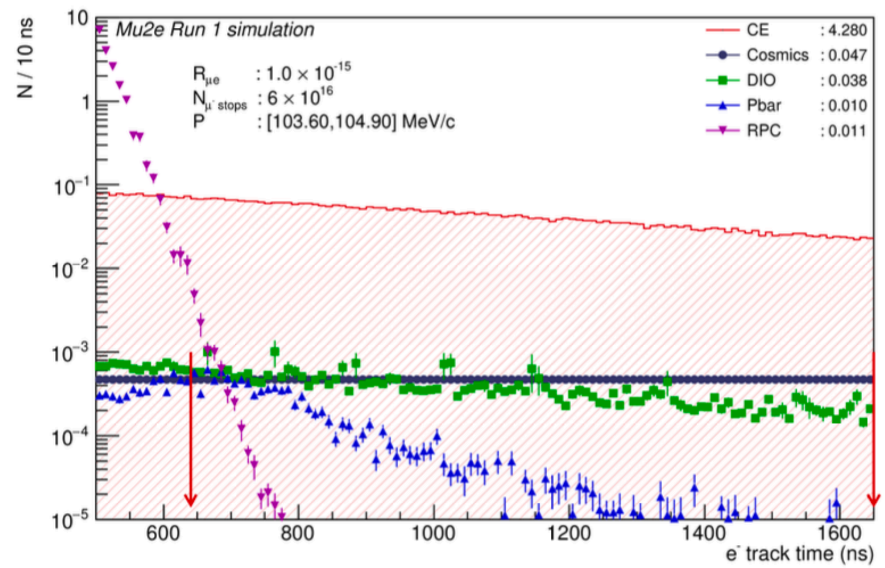

*Mu2e Collaboration MDPI Universe 2023 https://doi.org/10.3390/universe9010054

Physics data-taking plans

Run mode	Mean proton pulse intensity	Run time (s)	N(POT)	N(stopped muons)
Low intensity	1.6×10^{7}	9.5×10^{6}	2.9×10^{19}	4.6×10^{16}
High intensity	3.9×10^{7}	1.6×10^{6}	9.0×10^{18}	1.4×10^{16}
Total		11.1×10^{6}	3.8×10^{19}	6.0×10^{16}

Run I (2026-27)

1×10^{-15} 5σ discovery,

Single-Event-Sensitivity = 2×10^{-16}

Upper limit: 6×10^{-16} (90% C.L),

$10^{3} \times$ current limit

Run I + II

2×10^{-16} 5σ discovery,

Single-Event-Sensitivity = 3×10^{-17}

Upper limit: 8×10^{-17} (90% C.L),

$10^{5} \times$ current limit

Status: Solenoids

- **Production Solenoid:** Undergoing final tests. Delivery to Fermilab expected mid-2024.
- **Transport Solenoid:** Installed in the Mu2e hall.
- **Detector Solenoid:** Undergoing final tests. Delivery to Fermilab expected mid/late-2024.

Status: Detectors

Status: Detectors

- **Tracker:**

-> All 20736 straws produced.
-> All 216 panels produced. Now working through QC.
-> 33/36 planes are built.
-> Cosmic ray tests carried out with a single plane.

Status: Detectors

- **Tracker:**

  -> All 20736 straws produced.
  -> All 216 panels produced. Now working through QC.
  -> 33/36 planes are built.
  -> Cosmic ray tests carried out with a single plane.

- **Calorimeter:**

  -> Both disks have crystals and SiPMs installed.
  -> Final cabling underway.Installation in hall in Autumn 2024.

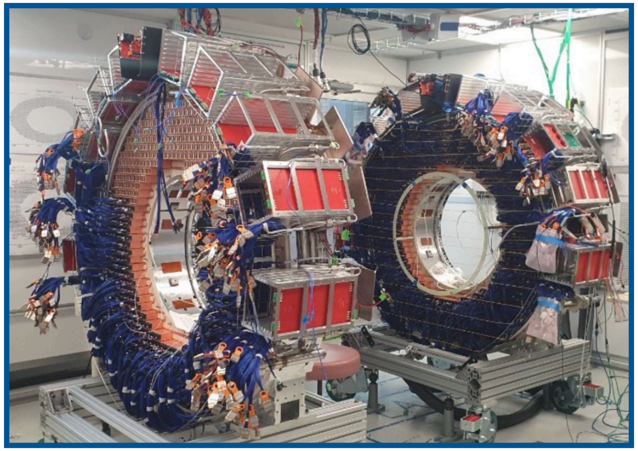

Status: Detectors

- **Tracker:**

  -> All 20736 straws produced.
  -> All 216 panels produced. Now working through QC.
  -> 33/36 planes are built.
  -> Cosmic ray tests carried out with a single plane.

- **Calorimeter:**

  -> Both disks have crystals and SiPMs installed.
  -> Final cabling underway.Installation in hall in Autumn 2024.

- **Cosmic Ray Veto:**

  -> All 5344 di-counters produced.
  -> All modules produced.
  -> Cosmic ray tests underway at Fermilab.

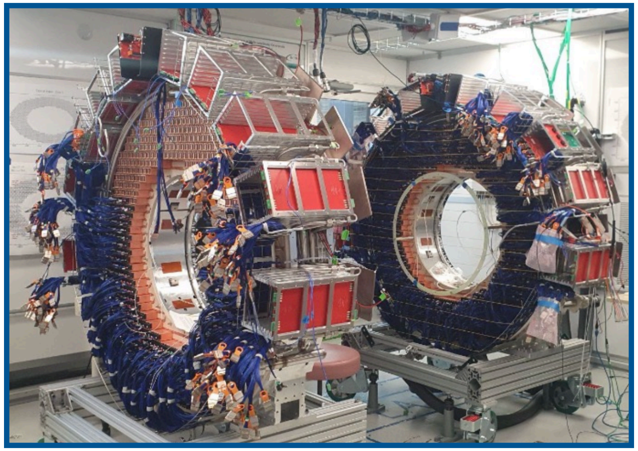

Conclusion

Conclusion

- Mu2e will search for the CLFV in muon to electron conversion with a 90% CL upper limit of < 8 x 10^{-17} .

Conclusion

- Mu2e will search for the CLFV in muon to electron conversion with a 90% CL upper limit of $< 8 \times 10^{-17}$.
- Muon CLFV channels offer deep indirect probes into BSM. Discovery potential over a wide range of BSM models.

Conclusion

- Mu2e will search for the CLFV in muon to electron conversion with a 90% CL upper limit of $< 8 \times 10^{-17}$.
- Muon CLFV channels offer deep indirect probes into BSM. Discovery potential over a wide range of BSM models.
- Mu2e commissioning with cosmics begins in 2025, commissioning with beam in 2026 and physics data taking follows.

Conclusion

- Mu2e will search for the CLFV in muon to electron conversion with a 90% CL upper limit of $< 8 \times 10^{-17}$.
- Muon CLFV channels offer deep indirect probes into BSM. Discovery potential over a wide range of BSM models.
- Mu2e commissioning with cosmics begins in 2025, commissioning with beam in 2026 and physics data taking follows.
- Looking further ahead the proposed Mu2e-II and AMF experiments will help elucidate any signal and push to higher mass scales.

Extra slides

CLFV with Muons: EFT Picture

$$\mathcal{L}_{\mathrm{CLFV}} = \overbrace{\boxed{\frac{m_\mu}{(1+\kappa)\Lambda^2}\bar{\mu}_R \sigma_{\mu\nu} e_L F^{\mu\nu}}}^{\text{Loop term}} + \overbrace{\boxed{\frac{\kappa}{(1+\kappa)\Lambda^2}\bar{\mu}_L \gamma_\mu e_L \left(\sum_{q=u,d} \bar{q}_L \gamma^\mu q_L\right)}}^{\text{Contact term}}$$

- Parameterize with dimension six EFT terms added to the SM Lagrangian ($\propto 1 / \Lambda^2$)
  - Loop term: e.g. SUSY, heavy ν's ...
  - Contact term: e.g. leptoquarks, heavy Z …
- **Mu2e sensitive to both types of terms***
- Λ mass scale -- **Mu2e will probe Λ~10^4 TeV**
- κ tunes relative contribution from each term

- Note that other EFT parameterizations exist
  [e.g. Davidson and Echenard DOI:10.1140/epjc/s10052-022-10773-4]

Loop term

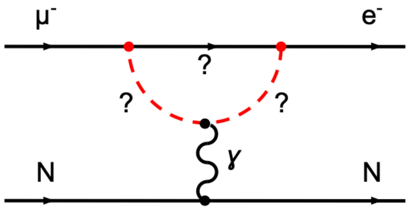

Contact term

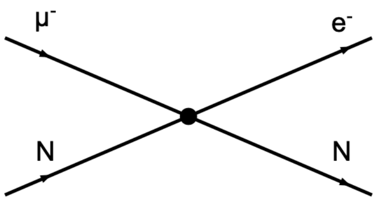

* There are 4 lepton contact operators that Mu2e is sensitive to at loop level, and Mu3e is sensitive to at leading order.

e.g.: $Br(\mu \to e\gamma) = \frac{3\alpha}{32\pi}\left|\sum_{i=2,3} U^*_{\mu i} U_{ei} \frac{\Delta m^2_{1i}}{M^2_W}\right|^2 < 10^{-54}$

[$U_{\alpha i}$ are the elements of the leptonic mixing matrix,
$\Delta m^2_{1i} \equiv m^2_i - m^2_1$, $i = 2, 3$ are the neutrino mass-squared differences]

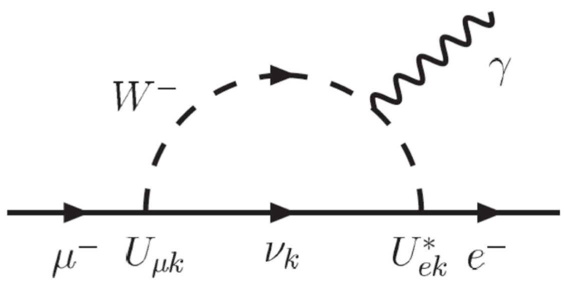

What does "Λ" mean?

This is clearly model dependent! However, some general issues are easy to identify…

- $\mu \to e\gamma$ always occurs at the loop level, and is suppressed by the E&M coupling e. Also chiral suppression (potential for "$\tan\beta$" enhancement).

$$\frac{1}{\Lambda^2} \sim \frac{e}{16\pi^2}\frac{\tan\beta}{M^2_{\rm new}}$$

- $\mu \to eee$ and $\mu \to e$-conversion in nuclei can happen at the tree-level

$$\frac{1}{\Lambda^2} \sim \frac{y^2_{\rm new}}{M^2_{\rm new}}$$

$N\mu^- \rightarrow Ne^-$: Complementarity in Target Materials

Overlap with nucleus probes form factors and reveals the nature of the interaction.

→ can elucidate type of physics through looking at relative conversion rate.

	S	D	V¹	V²
$\frac{B(\mu\to e,\mathrm{Ti})}{B(\mu\to e,\mathrm{Al})}$	$1.70 \pm 0.005_y$	1.55	1.65	2.0
$\frac{B(\mu\to e,\mathrm{Pb})}{B(\mu\to e,\mathrm{Al})}$	$0.69 \pm 0.02_{\rho_n}$	1.04	1.41	$2.67 \pm 0.06_{\rho_n}$

y = nuclear scalar form factor, ρ_n = nuclear neutron density

Higher Z target provides most splitting!

Kitano et al 2002: arXiv:hep-ph/0203110v

$$\mathrm{BR}(\mu \to e) \propto |DC_{DL} + S^pC^p_{S,L} + V^pC^p_{V,R} + S^nC^n_{S,L} + V^nC^n_{V,R}|^2 + (L \leftrightarrow R)$$

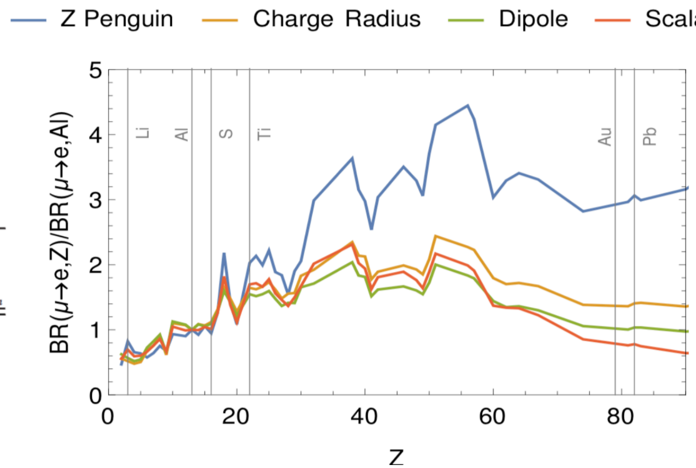

Mu2e: Why Al?

Practical Advantages	Physics Advantages
Chemically Stable	Conversion energy such that only tiny fraction of photons produced by muon radiative capture.
Available in required size/shape/thickness	Muon lifetime long compared to transit time of prompt backgrounds.
Low cost	Conversion rate increases with atomic number, reaching maximum at Se and Sb, then drops. Lifetime of muonic atoms decreases with increasing atomic number.
	Lifetime of muonic atom sits in "goldilocks" region i.e. neither longer than 1700 ns pulse spacing and greater than our pionic live gate.

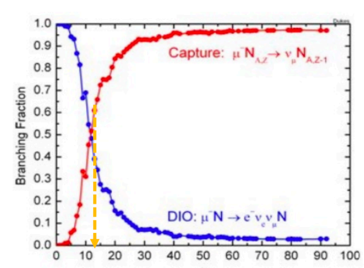

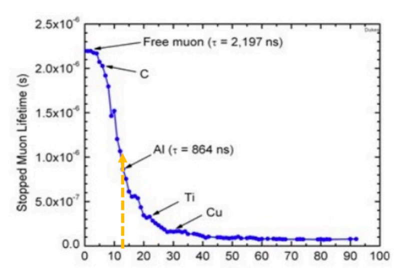

The lifetime of a muon in a muonic atom decreases with increasing atomic number.

Complementarity amongst channels

- All three channels are sensitive to many New Physics models.
- Relative Rates however will be model dependent and can be used to elucidate the underlying physics.

Mode	$\mu^+ \to e^+ e^+ e^-$	$\mu^- N \to e^- N$	$\frac{BR(\mu^+ \to e^+ e^+ e^-)}{BR(\mu^+ \to e^+ \gamma)}$	$\frac{BR(\mu^- N \to e^- N)}{BR(\mu^+ \to e^+ \gamma)}$
MSSM	Loop	Loop	~ 6 x 10^{-3}	10^{-3} – 10^{-2}
Type I Seesaw	Loop	Loop	3 x 10^{-3} – 0.3	0.1-10
Type II Seesaw	Tree	Loop	(0.1 – 3) x 10^{3}	10^{-2}
Type III Seesaw	Tree	Tree	~10^{3}	10^{3}
LFV Higgs	Loop	Loop	10^{-2}	0.1
Composite Higgs	Loop	Loop	0.05-0.5	2-20

Nucl. Phy. B (Proc. Suppl.) 248–250 (2014) 13–19

For example:

- In seesaw models CLFV rates aren't suppressed by smallness of neutrino mass.
- Different seesaw models give very different predicted rates of CLFV.
- **Measuring CLFV can help us understand neutrino mass origin!**

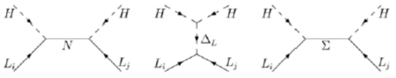

Complementarity with collider searches for CLFV

- Less stringent limits in 3rd generation, but here BSM effects may be higher.
- τ LFV searches at Belle II will be extremely clean, with very little background (if any), thanks to pair production and double-tag analysis technique.
- **To determine type of mediator:**
  - Compare muon channels to each other.
- **To determine the source of flavor violation:**
  - Compare muon rates to tau rates.

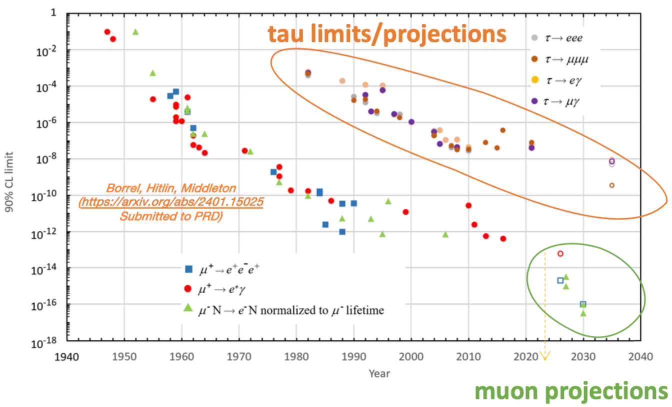

Targets

Production target: resides in Production Solenoid, stops 8 GeV protons, produces pions.

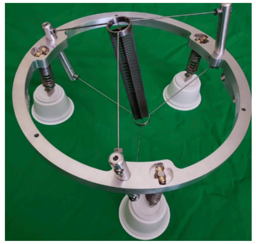

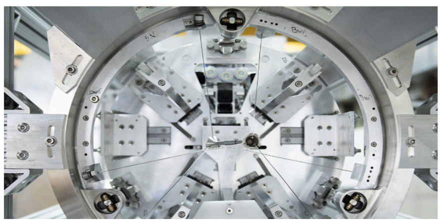

Muon Stopping target: resides in Detector Solenoid, stops muons, potentially produces signal conversion electrons.

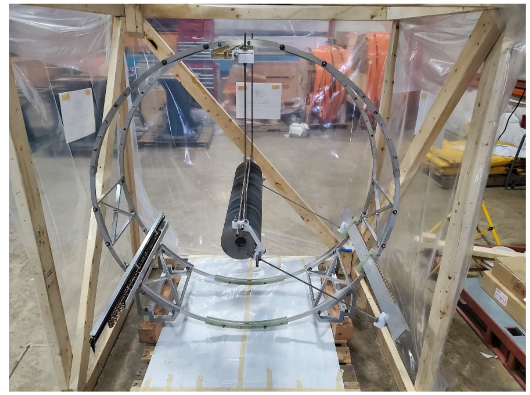

$N\mu^- \rightarrow Ne^-$: Signal

- Monoenergetic electron emanating from thin foil target with pile-up filtered out using existing Mu2e algorithms:

Mu2e/Mu2e-II Extinction

- Extinction is measure of out-of-time beam
- Mu2e-II requires extinction < 10^{-11}
  - cf Mu2e requirement < 10^{-10}
- Two factors contribute to extinction: intrinsic accelerator extinction, and AC resonant dipole sweepers
- Mu2e AC dipoles sweep away out-of-time protons into collimators– plan to use also for Mu2e-II
- PIP-II Linac extinction specification is 10^{-4-} -Likely will be better
- Expect improved performance from AC dipole for Mu2e-II (10^{-9} with safety margin)
  - Lower momentum means larger deflection
  - No beam halo from Mu2e's slow extraction septum
  - Lower momentum means lower punch through at collimator

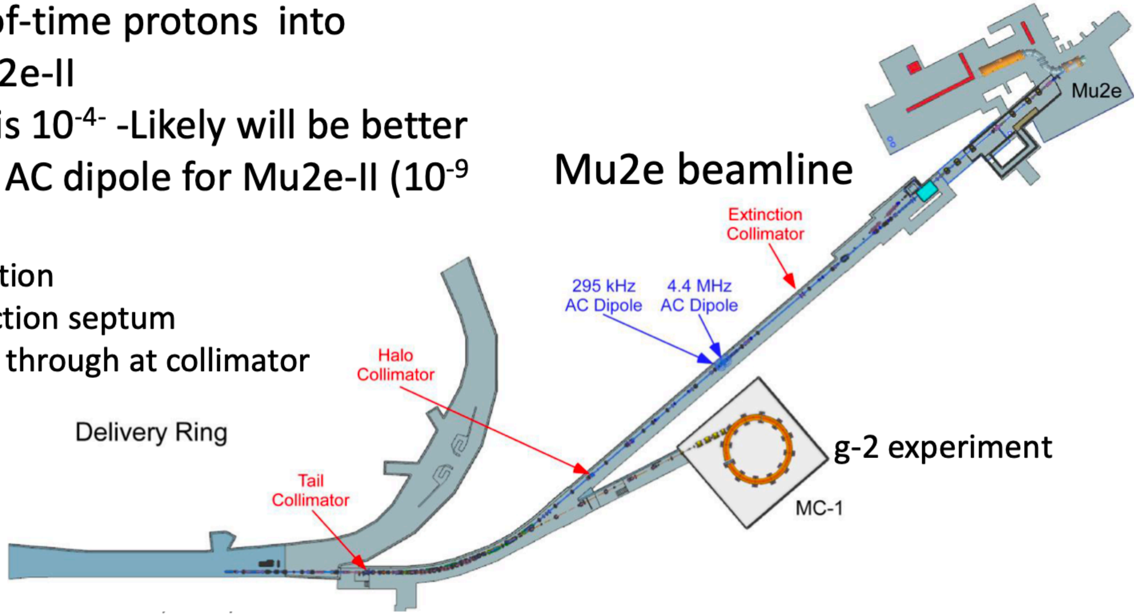

Timelines

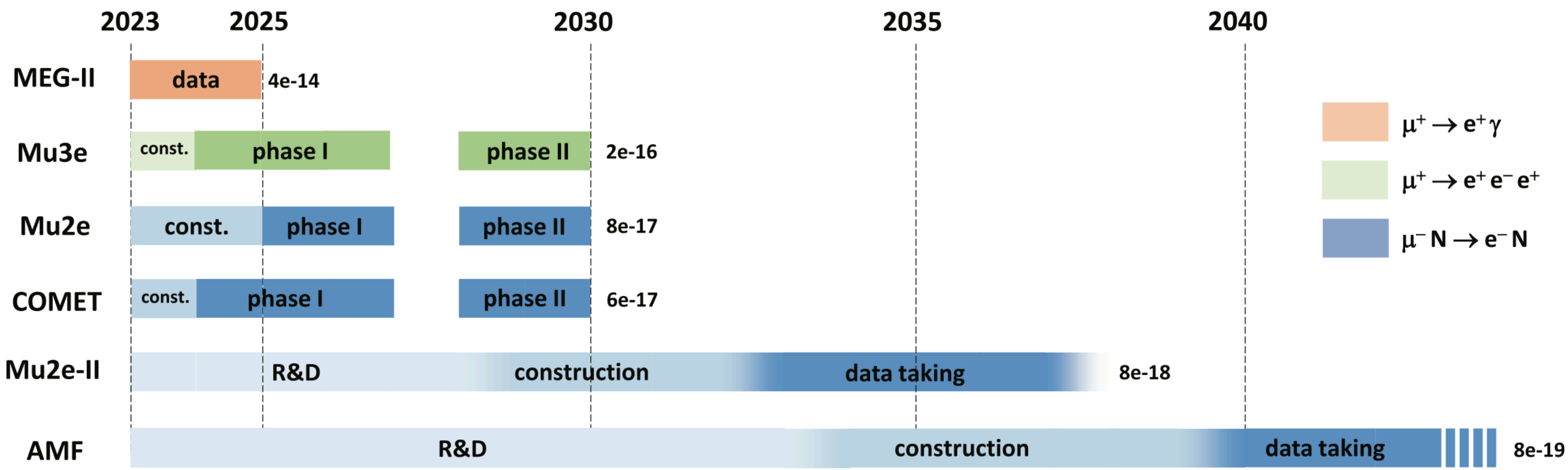

2023
2025
2030
2035
2040
MEG-II
data
4e-14
Mu3e
const.
phase I
phase II
2e-16
Mu2e
const.
phase I
phase II
8e-17
COMET
const.
phase I
phase II
6e-17
Mu2e-II
R&D
construction
data taking
8e-18
AMF
R&D
construction
data taking
8e-19
$\mu^+ \to e^+ \gamma$
$\mu^+ \to e^+ e^- e^+$
$\mu^- N \to e^- N$

STM: to measure the stopped muon rate

- Captured muons normalize the cLFV measurement.
- Captured muons can emit characteristic Al X-rays.
- Captured muons are measured by reconstructing the ^{27}Al X-ray energy spectrum.
- Captured muons = 60.9% of Stopped muons

STM: Reconstructs ^{27}Al energy spectrum.

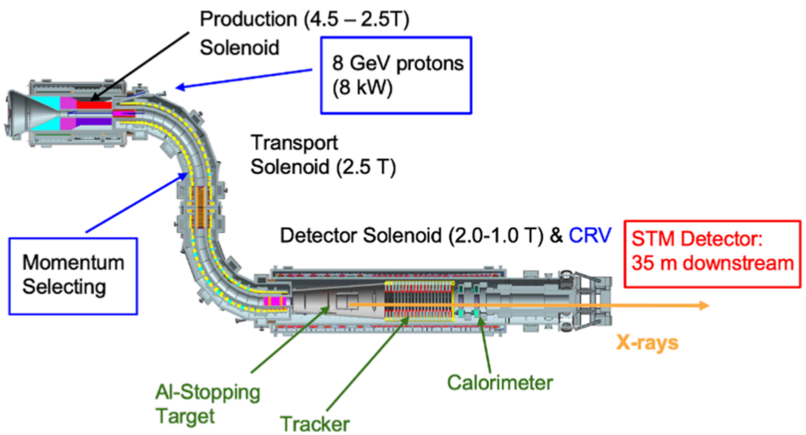

High Purity Germanium (HPGe) Detector.

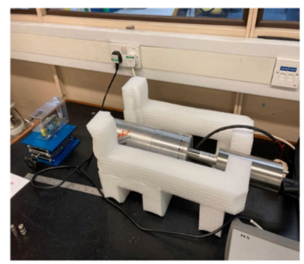

Corrected by STM acceptance